

AD-A048 896

AIR FORCE INST OF TECH WRIGHT-PATTERSON AFB OHIO SCH--ETC F/G 20/5
FLOW CHARACTERISTICS IN A TWO-DIMENSIONAL MULTIPLE-NOZZLE MULTI--ETC(U)
DEC 77 J L KINER

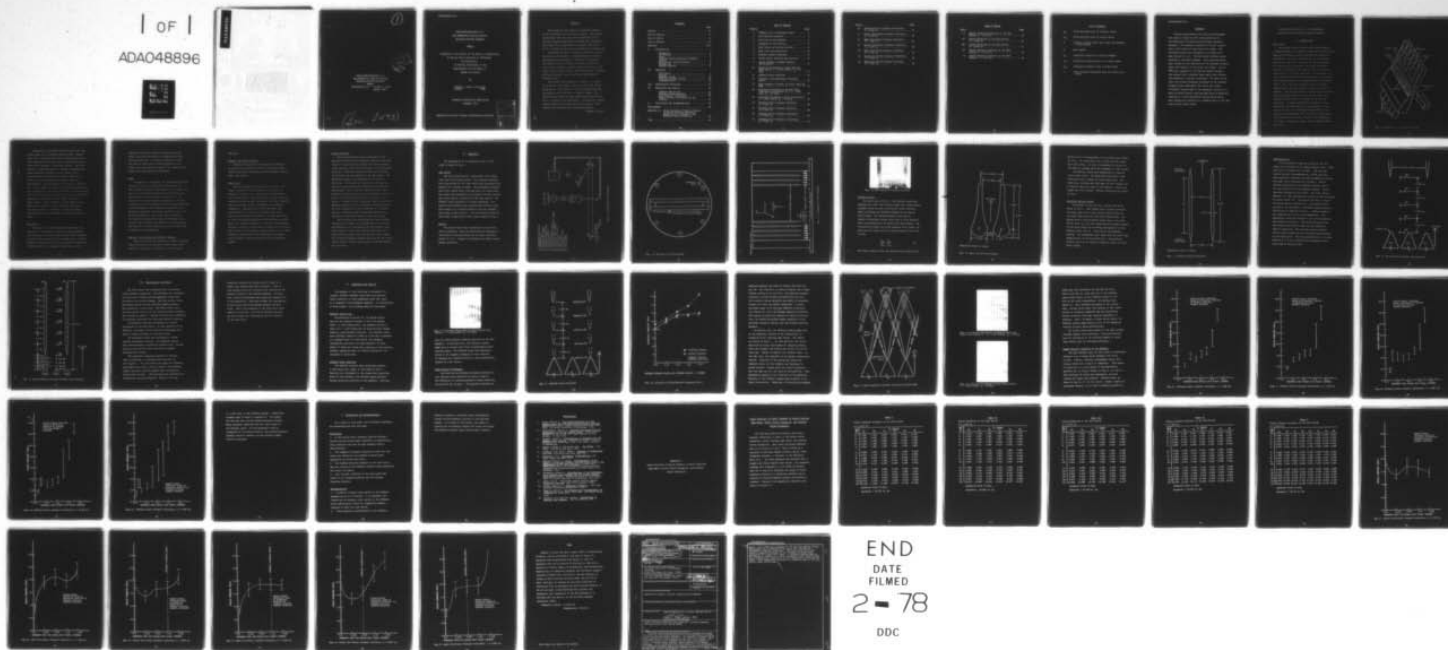
UNCLASSIFIED

AFIT/GAE/AA/77D-5

NL

| OF |

ADA048896



END
DATE
FILMED
2 - 78
DDC

①

DDC
JAN 23 1978
RESOLVED
F

FLOW CHARACTERISTICS IN A
TWO-DIMENSIONAL MULTIPLE-NOZZLE
MULTIPLE-DIFFUSER ASSEMBLY
THESIS

AFIT/GAE/AA/77D-5 Jeffrey L. Kiner
Captain USAF

(See 1473)

FLOW CHARACTERISTICS IN A
TWO-DIMENSIONAL MULTIPLE-NOZZLE
MULTIPLE-DIFFUSER ASSEMBLY

THESIS

Presented to the Faculty of the School of Engineering
of the Air Force Institute of Technology
Air University
in Partial Fulfillment of the
Requirements for the Degree of
Master of Science

by

Jeffrey L. Kiner, B.S.A.A.E.
Captain USAF

Graduate Aeronautical Engineering
December 1977

Approved for public release; distribution unlimited.

AFIT/GAE/AA/77D-5		
THIS	W. H. Section <input checked="" type="checkbox"/>	
DO	B. H. Section <input type="checkbox"/>	
NATHANIEL D		
JULIA D. D. D.		
BY		
DISTRIBUTION/AVAILABILITY CODES		
101	102	103
A		

Preface

This study was the result of continued interest in the development of high energy lasers. The overall requirements for this study were established by the Air Force Weapons Laboratory, Kirtland AFB, New Mexico. This study is a continuation of previous efforts by Dr. A. J. Shine of the Air Force Institute of Technology.

This study was made to observe variations in start and unstart performance in a multiple-nozzle variable multiple-diffuser assembly. Additional information was obtained on the variation of static pressures in the diffuser passages, nozzle trailing edge wakes, and nozzle center stream flows. Schlieren optical techniques and static pressure taps were the primary means of obtaining data.

The support and suggestions of Drs. A. J. Shine, W. C. Elrod, H. E. Wright, and R. A. Merz were deeply appreciated. The assistance of Mr. William Baker was invaluable, and he receives a special thanks. The apparatus for this study was expeditiously provided by Mr. M. W. Wolfe, AFIT shop formen. And finally, special acknowledgment is extended to my wife, Wandee, whose patience and devotion made this study possible.

Jeffrey L. Kiner

Contents

	Page
Preface	ii
List of Figures	iv
List of Tables	vi
List of Symbols	vii
Abstract	viii
I. Introduction	1
Background	1
The Problem	3
Scope	4
Variable Position Multiple Diffuser Defined	4
Started Test Cavity Defined	5
Assumptions	5
General Approach	6
II. Apparatus	7
Test Cavity	7
Nozzles	7
Diffuser Design	11
Schlieren Optical System	13
Instrumentation	15
III. Experimental Procedure	18
IV. Discussion and Results	20
Diffuser Throat Area	20
Diffuser Plane Positions	20
Start-Unstart Performance	21
Static Pressure Variations in the Diffuser	27
V. Conclusions and Recommendations	34
Bibliography	36
Appendix A: Axial Variation of Static Pressure in Nozzle Trailing Edge Wakes, Nozzle Center Streamline, and Diffuser Center Streamline	37
Vita	50

List of Figures

Figures		Page
1	Schematic of a Gas Dynamic Laser	2
2	Test Facility Schematic	8
3	Top View of Test Assembly	9
4	Schematic of Test Section	10
5	Test Cavity in Vertical Position	11
6	Mach 3.23 Contoured Nozzle	12
7	Diffuser Design Parameters	14
8	Center Nozzle Pressure Tap Locations	16
9	Center Diffuser and Wake Pressure Tap Locations	17
10	Schlieren Photograph of Fully Started Test Cavity, $L = 1.333$ inches, $P_o = 82$ psig	21
11	Diffuser Plane Positions	22
12	Variation of Start/Unstart Pressures with L	23
13	Shock Expansion Pattern at Nozzle Trailing Edge	25
14	Schlieren Photograph of Subsonic Wake from Nozzle Vane Number 20 , $L = 1.000$ inch, $P_o = 68$ psig	26
15	Schlieren Photograph of Full Cavity Start $L = 1.000$ inches, $P_o = 68$ psig	26
16	Diffuser Static Pressure Variation, $L = 1.333$ in.	28
17	Diffuser Static Pressure Variation, $L = 1.000$ in.	29
18	Diffuser Static Pressure Variations, $L = 0.667$ in.	30
19	Diffuser Static Pressure Variations, $L = 0.333$ in.	31

Figure		Page
20	Diffuser Static Pressure Variations, L = 0.000 in.	32
21	Nozzle Flow Static Pressure Variation, L = 1.333 in.	44
22	Wake Flow Static Pressure Variation, L = 1.333 in.	45
23	Nozzle Flow Static Pressure Variation, L = 1.000 in.	46
24	Wake Flow Static Pressure Variation, L = 1.000 in.	47
25	Nozzle Flow Static Pressure Variation, L = 0.667 in.	48
26	Wake Flow Static Pressure Variation, L = 0.667 in.	49

List of Tables

Table		Page
I	Static Pressure Variations in the Test Cavity, $L = 1.333$ in.	39
II	Static Pressures in the Test Cavity, $L = 1.000$ in.	40
III	Static Pressures in the Test Cavity, $L = 0.667$ in.	41
IV	Static Pressure Variation in the Test Cavity, $L = 0.333$ in.	42
V	Static Pressure Variation in the Test Cavity, $L = 0.000$ in.	43

List of Symbols

A_{dt}	Cross-sectional area of diffuser throat
A_{nt}	Cross-sectional area of nozzle throat
L	Distance between nozzle exit plane and diffuser entrance plane
M	Mach number
P_o	Stagnation pressure in stilling chamber
P_{ox}	Stagnation pressure prior to a normal shock
P_{oy}	Stagnation pressure after a normal shock
x	Axial distance downstream from the nozzle exit plane

Abstract

Pressure measurements and schlieren photographs were used to study the flow characteristics in a two-dimensional multiple-nozzle multiple-diffuser assembly. The assembly consisted of 29 full nozzles with a half nozzle at each end of the array. The contoured nozzles were designed for an ideal exit Mach number of 3.23 . Fourteen axial diffuser vanes provided 15 diffuser passages. Flow characteristics were studied at five positions of the diffuser entrance plane with respect to the nozzle exit plane. Air at 80°F and a maximum of 118 psig was passed through the nozzles into a constant area region then through the diffusers to ambient conditions. The test cavity start and unstart pressures decreased as the diffuser entrance plane approached the nozzle exit plane. A diffuser leading edge in the immediate vicinity of a major alternate nozzle trailing edge shock intersection resulted in a flow instability during cavity start. This instability resulted in a subsonic wake in the test cavity after cavity start.

FLOW CHARACTERISTICS IN A TWO-DIMENSIONAL MULTIPLE-NOZZLE MULTIPLE-DIFFUSER ASSEMBLY

I. Introduction

Background

The general class of high energy lasers employs a flowing medium as a means of producing non-equilibrium molecular vibrational energy populations, population inversions. The basic operation of the high energy chemical or gas dynamic laser is the rapid expansion of a gas through an array of very short supersonic nozzles. Depending on the type of laser, mixing may occur prior to or after expansion. In all cases, the result is that the molecular vibrational energy cannot relax rapidly enough to maintain Boltzmann equilibrium (ref 6, 12). As these molecules relax to a stable energy level, they may release energy in the form of photons. This photon release is referred to as lasing. By using optical mirrors to reflect the laser beam through the flow field, the power of the beam is amplified. A large amplification requires a large population inversion which in turn requires a large mass flow rate of the working medium (ref 9). One method of accomplishing this is to use a large array of closely spaced nozzles. Figure 1 is a schematic of a high energy laser system, the gas dynamic laser (ref 3:2).

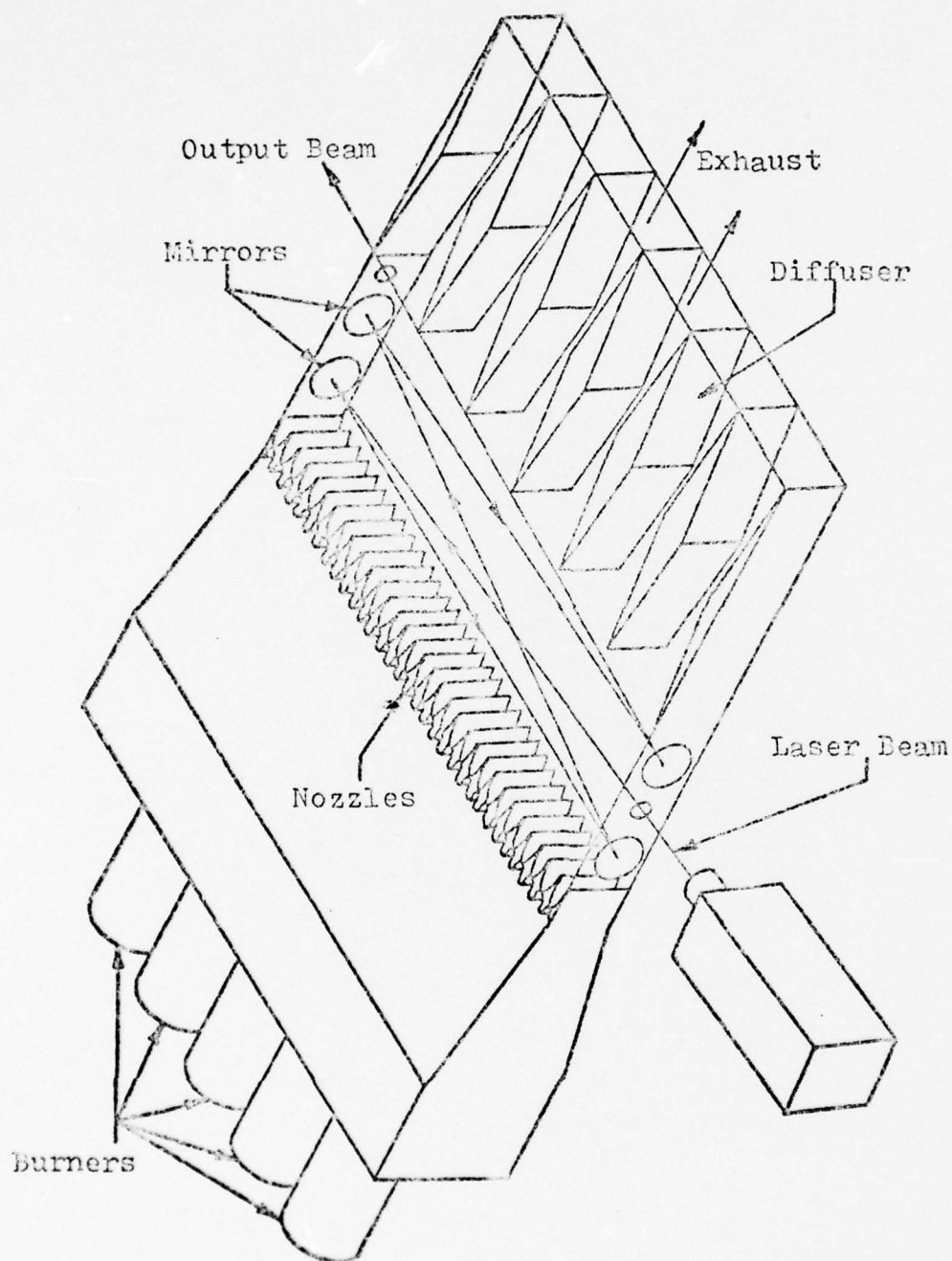


Fig. 1. Schematic of a Gas Dynamic Laser

Packaging is the primary problem facing the high energy laser as an aerospace weapon system. System mass, size, and operational power requirements tend to make starting and operation at the lowest practicable system inlet pressure a desirable feature. Low inlet pressure in turn may produce a pressure substantially below atmospheric pressure in the lasing cavity. Consequently, to discharge the flow, a diffuser or other means of increasing the pressure should be incorporated. The effectiveness with which a diffuser recovers the pressure depends on its design and pressure on the downstream side of the diffuser. Several studies (ref 2, 3, 7, 8) have been made in this area. Packaging requirements dictated that the diffuser occupy a small volume. Short diffusers in turn tend to drive system inlet pressures higher which in turn makes the system heavier. Therefore, a means of keeping inlet pressures low and diffuser volume small must be found.

The Problem

The purpose of this study was to determine if a cold flow, two-dimensional, multiple nozzle-diffuser assembly could be started and maintain stable operation at lower inlet pressures in an assembly with a variable diffuser entrance plane than in an assembly with fixed diffuser vanes. It attempted to show that as the

distance between the diffuser entrance plane and nozzle exit plane decreases, the required starting pressure decreases. It further attempted to show that some of these lower starting pressures were within the stable pressure range of the system in its steady state operational configuration.

Scope

In support of this study, the following objectives were met: (1) move the diffuser entrance plane to five specific locations with respect to the nozzle exit plane, L; (2) determine minimum starting pressure at each location of the diffuser entrance plane; (3) determine the minimum operating pressure of the test cavity at each of the diffuser entrance plane positions; and (4) determine static pressure variations in the streamwise direction at several locations in the test cavity and diffuser. This study did not address: (1) variation of specific heats; (2) boundary layer control; (3) boundary layer effects in the flow field; (4) variation of inlet temperature; nor (5) variation of diffuser exit conditions.

Variable Position Multiple Diffuser Defined

Variable position is defined as a series of steady state positions of the diffuser entrance plane with respect to the nozzle exit plane in the streamwise

direction.

Started Test Cavity Defined

Started test cavity is defined as the condition of steady state supersonic flow in the entire region between the nozzle exit plane and the diffuser entrance plane, the cavity.

Assumptions

Air was assumed to behave as an ideal gas. The ratio of specific heats was assumed to remain at a constant value of 1.40 . All nozzle inlet pressures were assumed equal. One-dimensional, steady, adiabatic, inviscid flow was assumed throughout the entire assembly after the cavity starts. The nozzles were assumed isentropic. Flow patterns in the test model were assumed similar to those in an actual high energy laser under operating conditions. The flow conditions at the five specific positions of the diffuser entrance plane were assumed identical to those in a continuously variable diffuser entrance plane at these same locations. The location of the diffuser entrance plane at $L = 1.333$ inches was assumed to be the steady state operating point of both a variable position and fixed diffuser system.

General Approach

Flow characteristics were determined at five specific locations of the diffuser entrance plane with respect to the nozzle exit plane from 0.000 inches to 1.333 inches in 0.333 inch increments in the streamwise direction. Schlieren optical methods were utilized to determine the flow pattern in the test model. The schlieren assembly was perpendicular to the flow direction. The nozzle exit plane, test cavity, and entire diffuser region were visible in the schlieren photographs. One set of five static pressure taps measured pressure variation in the streamwise direction along an axis coincident with the centerline of a nozzle. A second set of 11 pressure taps measured the pressure variation in the streamwise direction along an axis coincident with the centerline of a diffuser passage. Stilling chamber stagnation pressure was recorded at start and unstart of the test cavity.

The following test conditions were held constant throughout the study: (1) the geometry of the nozzles and diffusers; (2) the geometry of the diffuser vanes with respect to each other remained constant; (3) a thirty nozzle assembly was used for the entire study; (4) a fifteen diffuser assembly was used for the entire study; and (5) diffuser exit pressure remained ambient for all tests.

II. Apparatus

The arrangement of the apparatus used in this study is shown in Fig 2 .

Test Cavity

The test cavity was 8.1 inches wide, 9.95 inches long, and 0.375 inches across. The external sidewalls were constructed of 0.75 inch thick clear plexiglass and measures 11.1 inches in width. The plexiglass endwalls were 0.375 inches thick, and each was 1.50 inches wide. The nozzle bank consisted of 30 nozzles, 29 full nozzles and a half nozzle at each end of the test cavity. The diffuser bank consisted of 15 axial diffusers. The nozzles and diffusers were numbered from left to right with respect to a reference mark on the test assembly base plate, shown in Fig 3 . The test section used for this study is depicted in Fig 4 and is shown in Fig 5 .

Nozzles

The nozzle walls were constructed of 0.375 inch thick plexiglass. They were contoured and designed by the method of characteristics for an ideal exit Mach number of 3.23 . Figure 6 illustrates the basic nozzle design parameters.

1. Compressor and dryer
2. Storage tank
3. Flow control valve
4. Filters and screen
5. Chamber pressure tap
6. Stilling chamber
7. Test section
8. Static pressure taps
9. Static pressure manometer boards
10. Manometer data camera
11. Zirconium arc lamp
12. Spark lamp
13. Plane mirror
14. Parabolic mirror
15. Knife edge
16. Focal plane

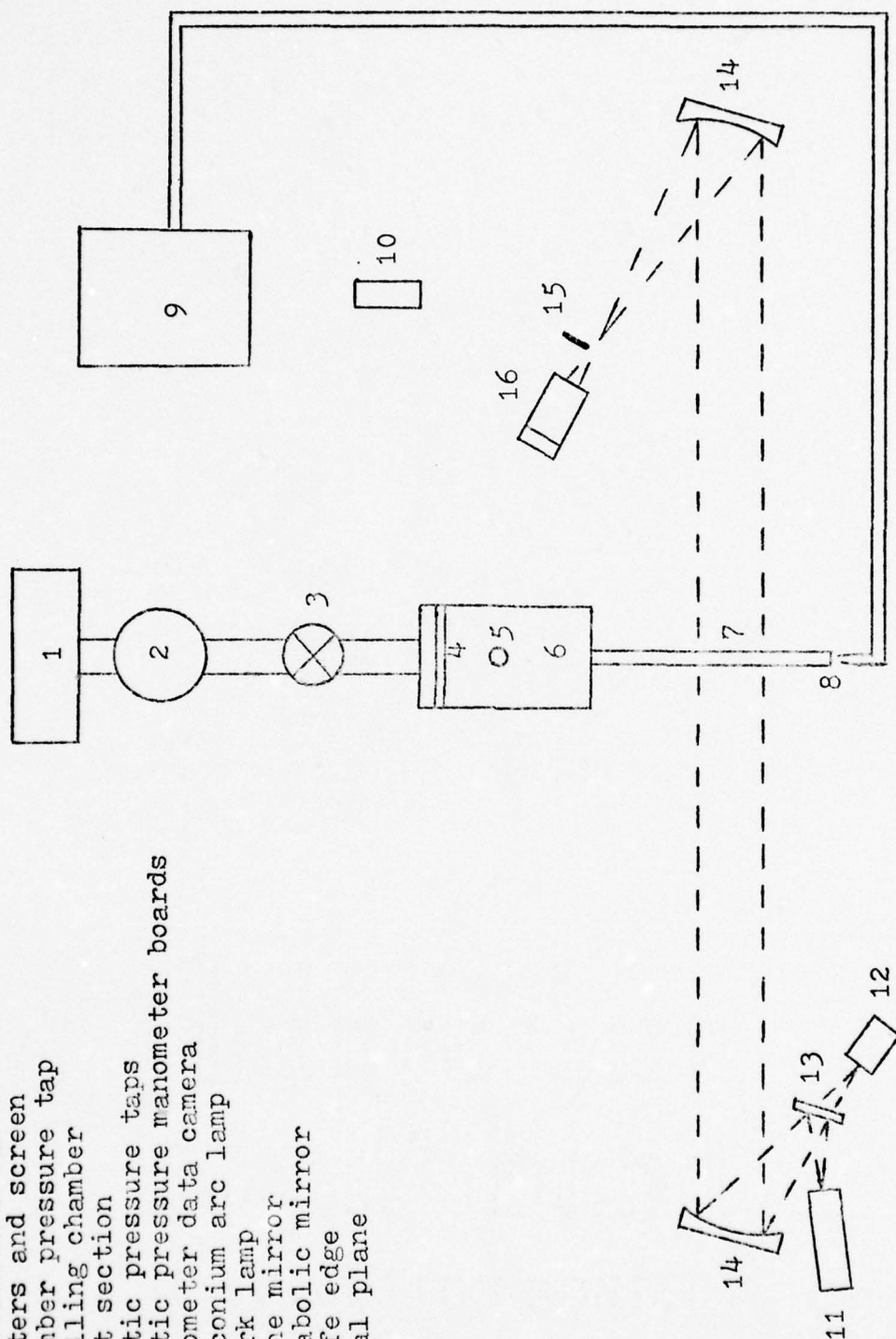


Fig. 2. Test Facility Schematic

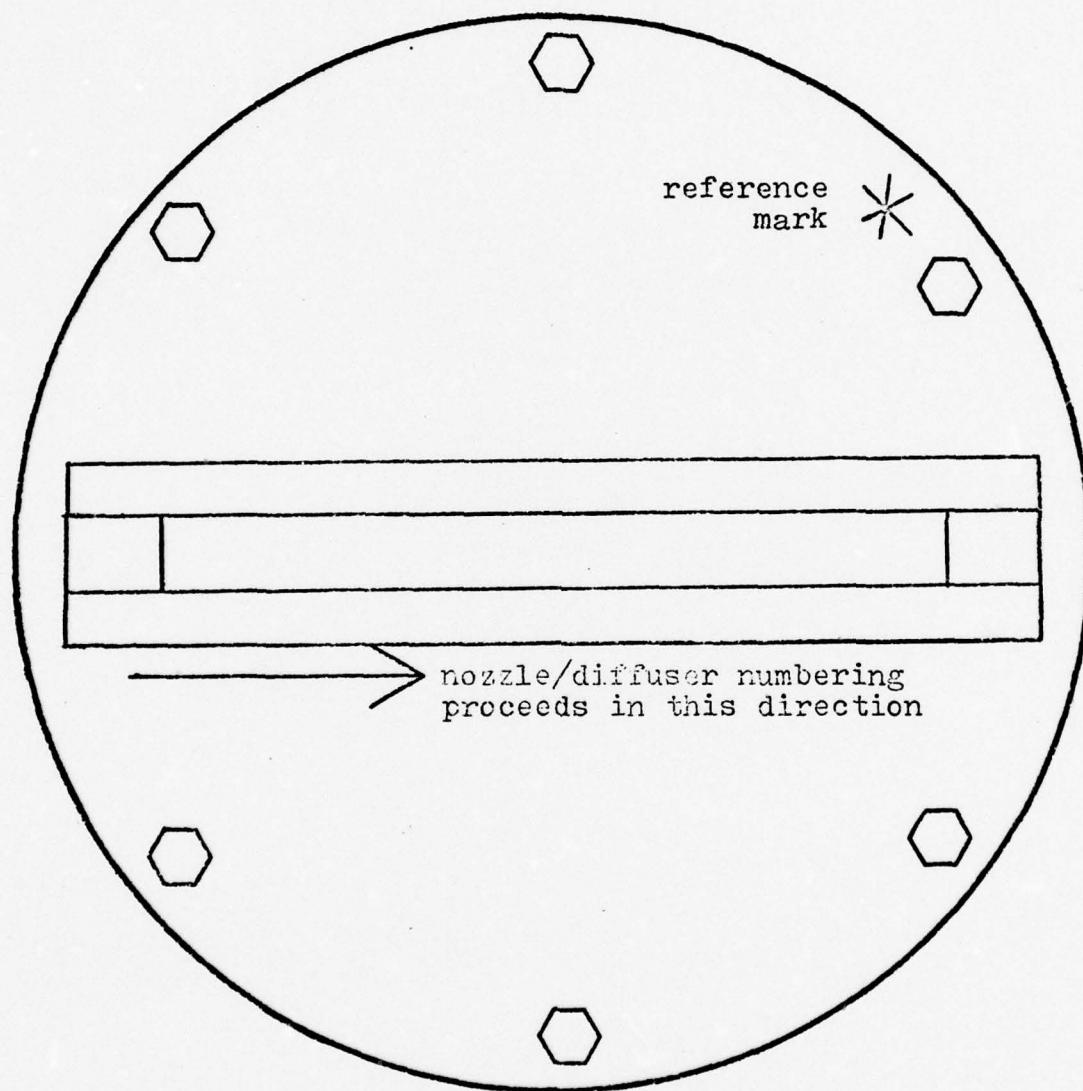


Fig. 3. Top View of Test Assembly

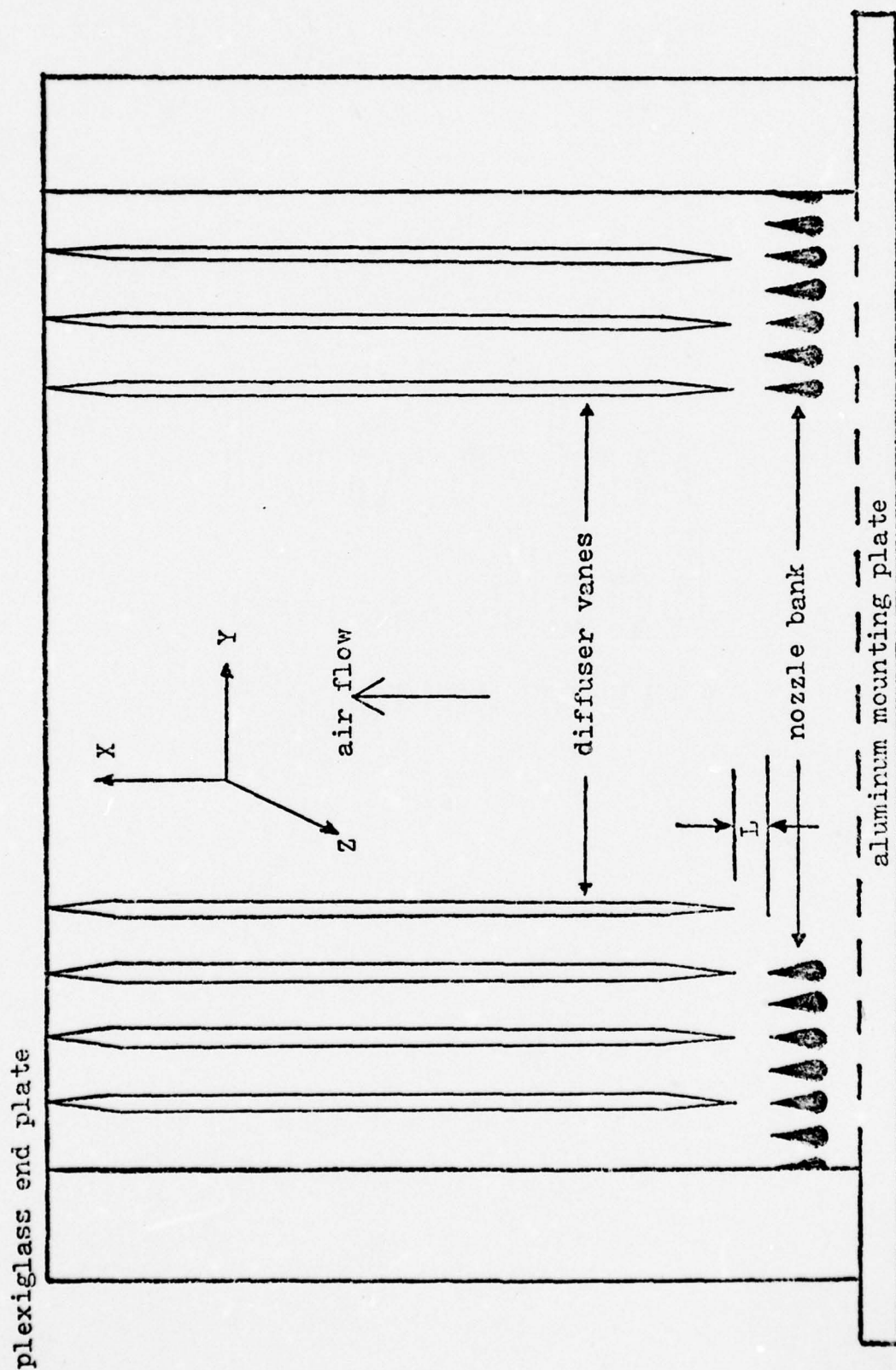


Fig. 4 . Schematic of Test Section

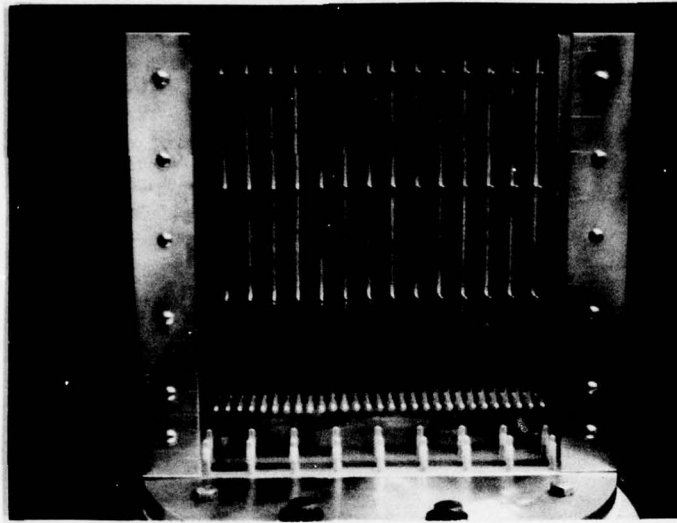


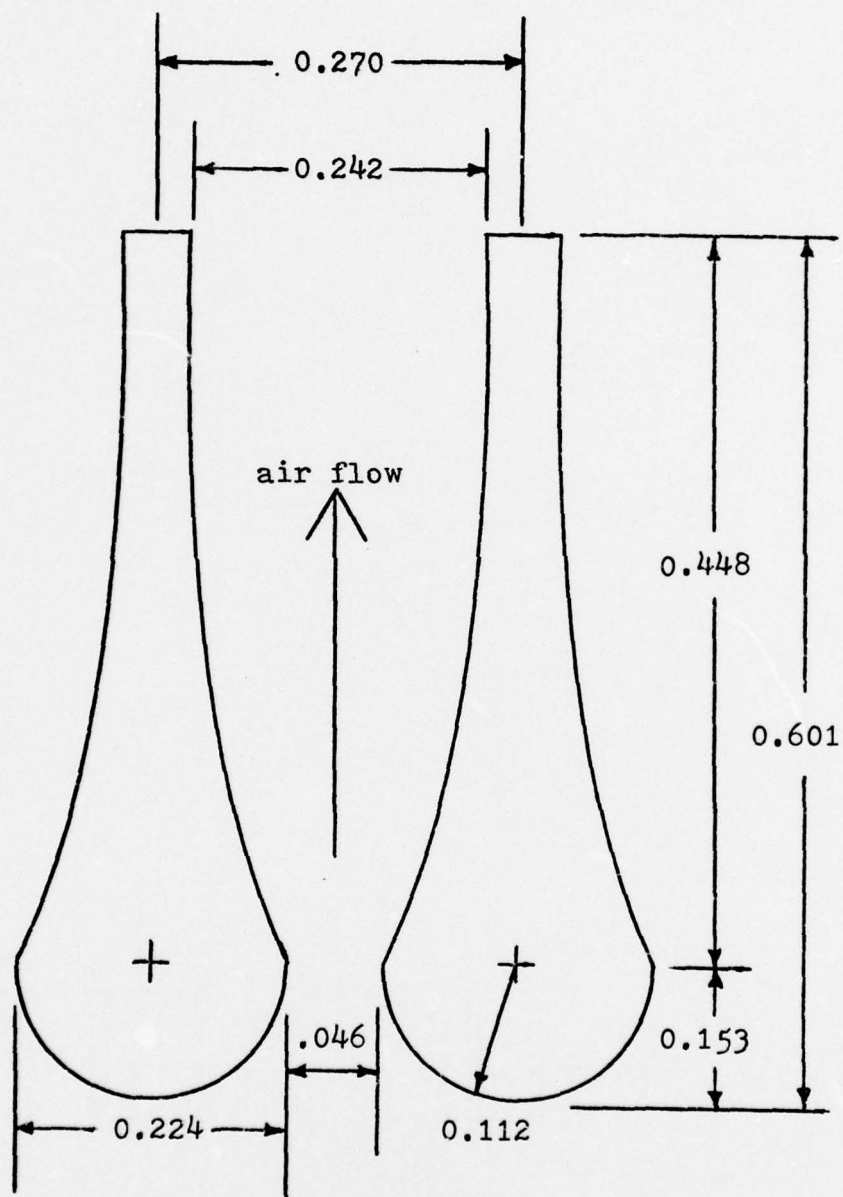
Fig. 5. Test Cavity in Vertical Position

Diffuser Design

As can be seen in Fig 4 , the diffuser vanes were arranged such that their leading edges were geometrically aligned along the axes of alternate nozzle trailing edges, providing one diffuser passage per two nozzle flow streams. The minimum diffuser area must be capable of passing a normal shock with a total pressure ratio as determined by the nozzle exit Mach number. The relationship between the total pressure ratio across the shock and the nozzle and exit throat areas is (ref 1:20, 11:144):

$$\frac{A_{nt}}{A_{dt}} = \frac{P_{oy}}{P_{ox}} \quad (1)$$

The total pressure ratio was obtained from normal shock



Dimensions shown in inches

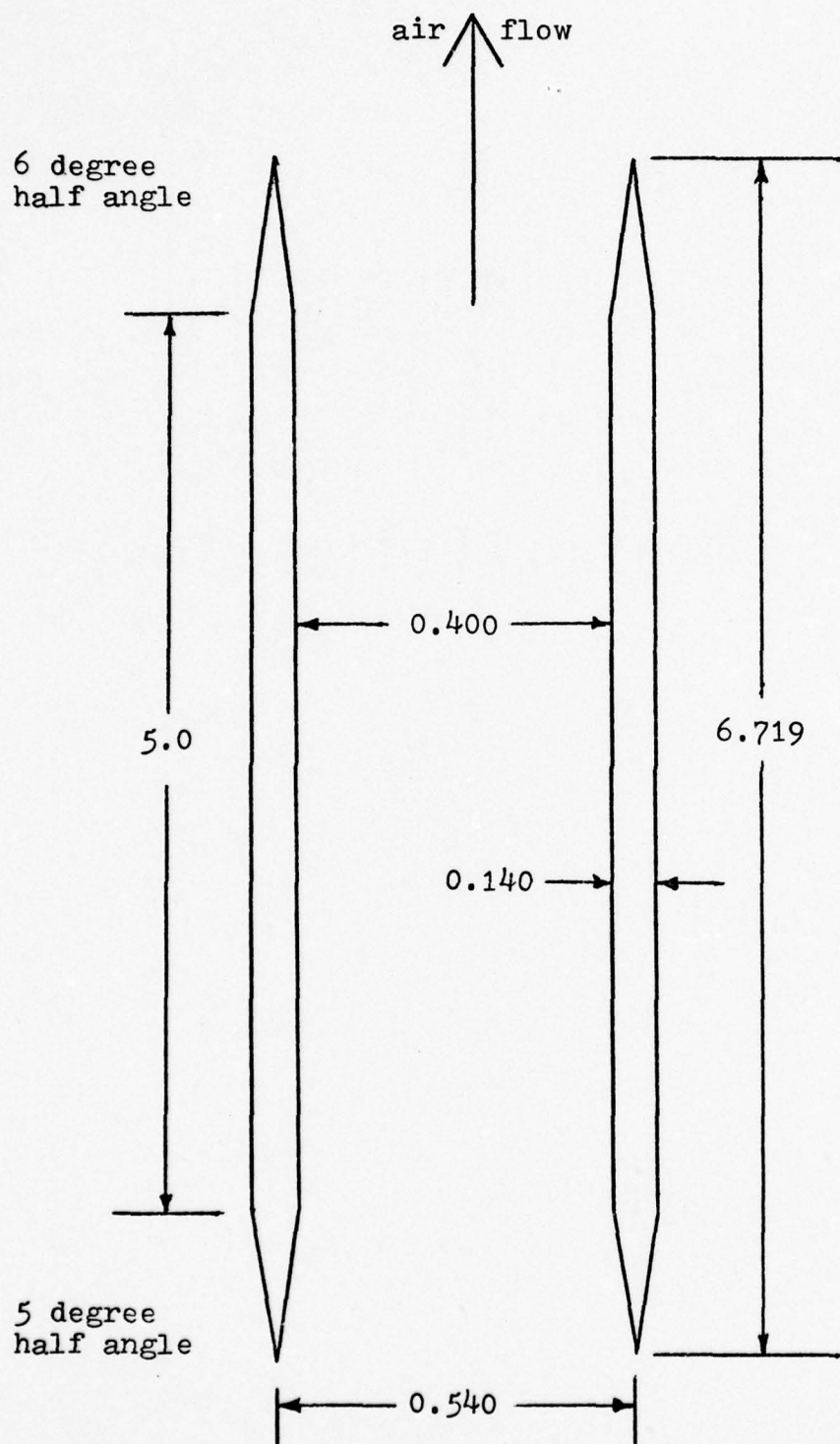
Fig. 6. Mach 3.23 Contoured Nozzle

tables (ref 4) corresponding to an entrance Mach number of 3.23 . The resulting ideal minimum diffuser width was 0.342 inches. As will be discussed in section IV, the diffuser passage width was enlarged to 0.400 inches.

The diffuser vanes were constructed of aluminum 0.375 inches thick. The vanes were originally 0.199 inches and later reduced to 0.140 inches wide. The vanes had a leading edge half angle of five degrees and a trailing edge half angle of six degrees. Total vane length was 6.719 inches. Diffuser dimensions are shown in Fig 7 .

Schlieren Optical System

A schematic of the schlieren optical system is shown in Fig 2 . This system used a steady zirconium arc lamp light source and a frosted glass screen at the focal plane for real time flow observations. The system used a 1/6 microsecond spark lamp as the light source and a (4 x 5) inch format Polaroid graphic camera at the focal plane for recording photographic results. Polaroid film, type 47 , was used for photographic results. All photographs were taken with the knife edge perpendicular to the flow direction. The parabolic mirrors used were 16 inches in diameter with a 72 inch focal length.



Dimensions shown in inches

Fig. 7. Diffuser Design Parameters

Instrumentation

A 0-200 psig dial gage was located in the air supply line upstream of the supply control valve. This gage had an accuracy of ± 1.0 psi . The stilling chamber pressure was measured on a 0-100 psig dial gage physically located on one of the manometer boards. This gage had an accuracy of $\pm 1/2$ psi . Static pressure measurements were obtained through taps in the test section's rear plexiglass sidewall. These taps were arranged in two series. The first series, numbers 1-5 , was geometrically located on the centerline of nozzle number 16 . This series is shown in Fig 8 . The second series, numbers 6-16 , was geometrically located on the centerline of diffuser passage number 5 . This series is depicted in Fig 9 . Static pressures were measured on 50 inch U-tube manometers. The manometers, which were scaled in 0.10 inch increments, were mounted vertically. They contained mercury as the working fluid and the free end was exposed to ambient conditions. The stilling chamber pressure and all static pressures were recorded simultaneously at each data point. This was accomplished by a tripod mounted (4 x 5) inch format Polaroid graphic camera using type 42 Polaroid film.

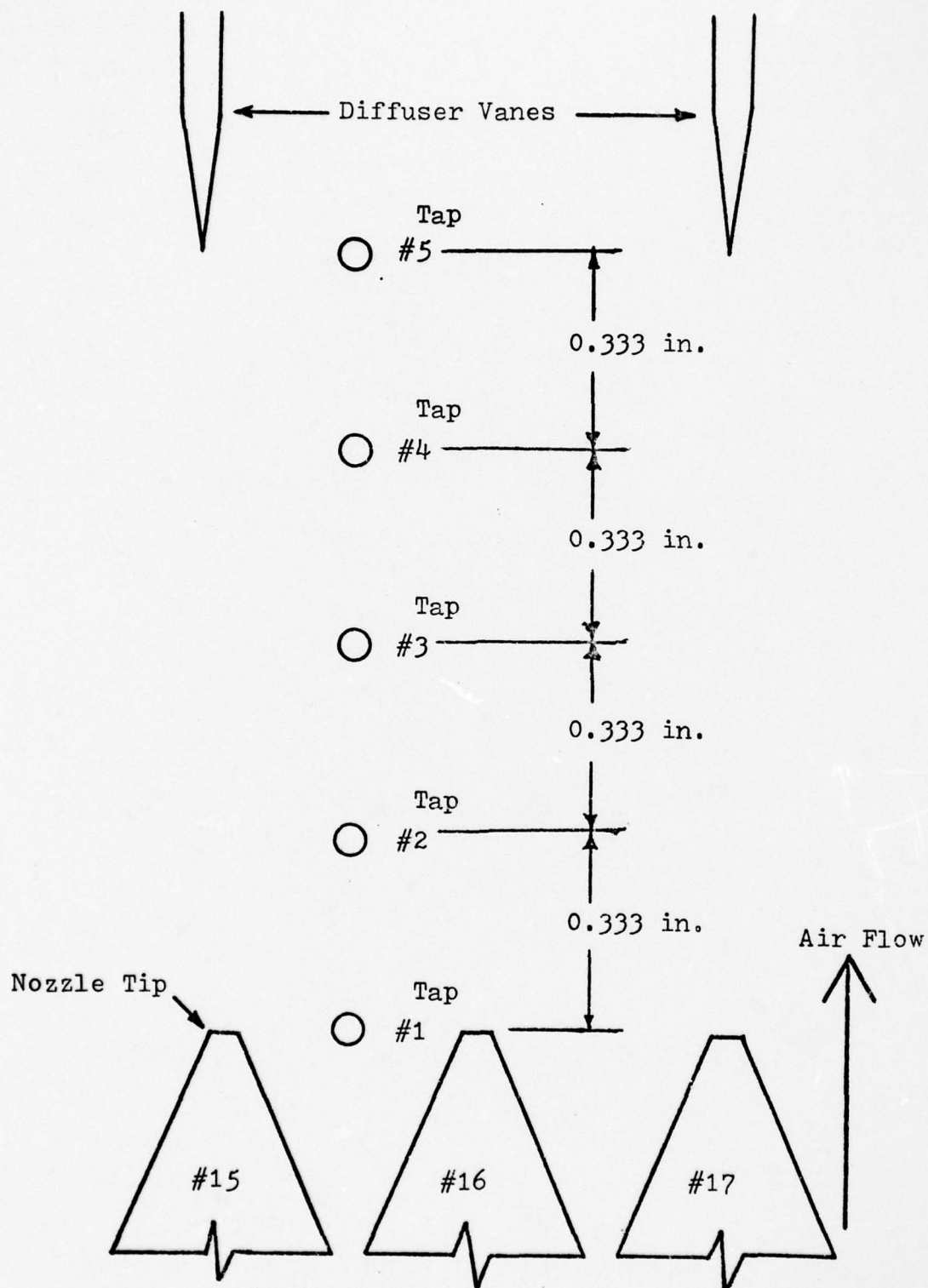


Fig. 8. Center Nozzle Pressure Tap Locations

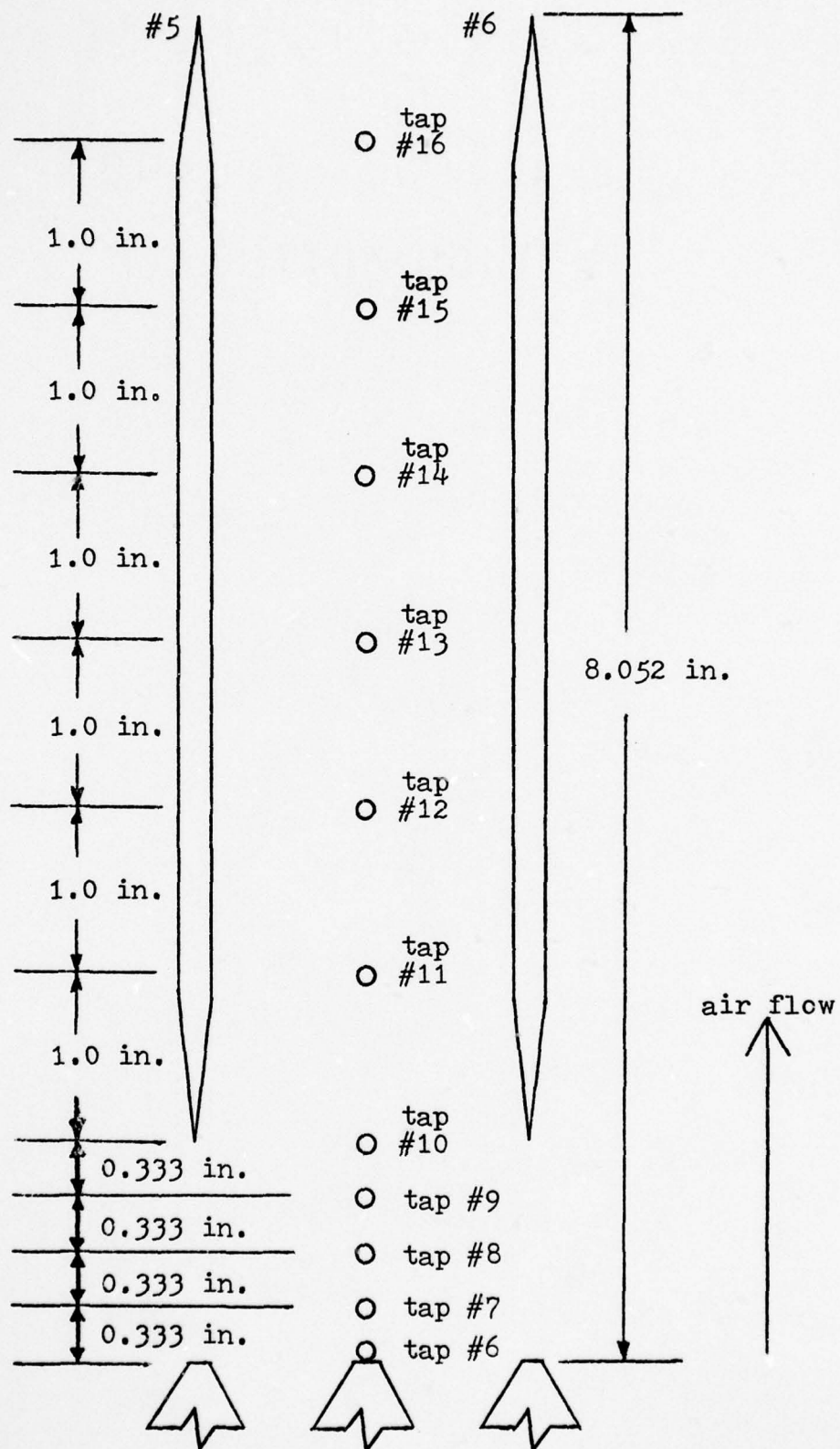


Fig. 9. Center Diffuser and Wake Pressure Tap Locations

III. Experimental Procedure

The test section was configured with the desired nozzle-diffuser separation. The schlieren was configured for continuous viewing, and the manometer boards were positioned for optimum viewing. The flow control valve was slowly opened, and the stilling chamber pressure was recorded at cavity start. The flow control valve was then slowly closed, and the stilling chamber pressure was recorded at unstart. Several test runs were conducted to accurately determine the start and unstart pressures.

The schlieren was then reconfigured to obtain photographs of the flow field. At each position of the diffuser, a minimum of five schlieren photographs were taken to assure accuracy of flow field data.

The manometer boards were realigned to obtain optimum photographic results. All manometer values were instantaneously recorded on Polaroid film. Several pictures were taken at each data point to assure repeatability of data.

The compressor supplied a maximum of 118 psig which corresponds to a maximum mass flow rate of $0.55 \text{ Lb}_m/\text{sec}$. The test cavity was capable of handling much higher flow rates, and as a result, the stilling chamber pressure bled off rapidly above 75 psig and slowly below 65 psig. This provided some difficulty in determining starting pressures. However, this was

beneficial because the system could be taken to a higher than desired data point pressure. Then as line pressure bled off, pictures were obtained of the manometer boards at the desired pressure. By doing this, starting transients were completely dampened out of the manometers. This also allowed the experimenter to move freely about and closely observe the flow field. Hence, any anomalies in the flow field could readily be detected. The rate of pressure decrease was slow enough that disturbances were not induced in the flow field.

IV. Discussion and Results

The purpose of this study was to determine if a variable diffuser assembly could start and maintain stable operation at inlet pressures lower than those in a comparable fixed diffuser assembly. In consideration of this purpose, the following items are discussed.

Diffuser Throat Area

As mentioned in section II, the design throat area for the diffuser yielded a 0.342 inch passage width. At this design point, the assembly would not start at $L = 1.333$ inches and 100 psig stilling chamber pressure, peak pressure available. The diffuser vanes were uniformly reduced in width in 0.002 inch increments. At a passage width of 0.400 inches, the assembly consistently started at the same pressure, 82 psig. Figure 10 shows the cavity fully started at this position. Diffuser parameters were not further altered for the remainder of this study.

Diffuser Plane Positions

The diffuser entrance plane positions relative to the nozzle exit plane, L , are shown in Fig 11. Position one corresponds to the steady state operating point of this assembly, the diffuser plane position during continuous operation of the assembly. This was



Fig. 10. Schlieren Photograph of Fully Started Test Cavity, $L = 1.333$ inches, $P_o = 82$ psig

also the fixed diffuser reference position of the test assembly. At position five, the diffuser leading edges were in contact with their corresponding nozzle trailing edges. The diffuser vanes were physically bolted to the assembly sidewalls at each position. In changing the diffuser position, L was consecutively reduced by 0.333 inches.

Start-Unstart Performance

The start and minimum operating pressures at each diffuser plane position are shown in Fig 12 . The difference in starting pressures between positions one and five was 35 psig . The greatest reduction in

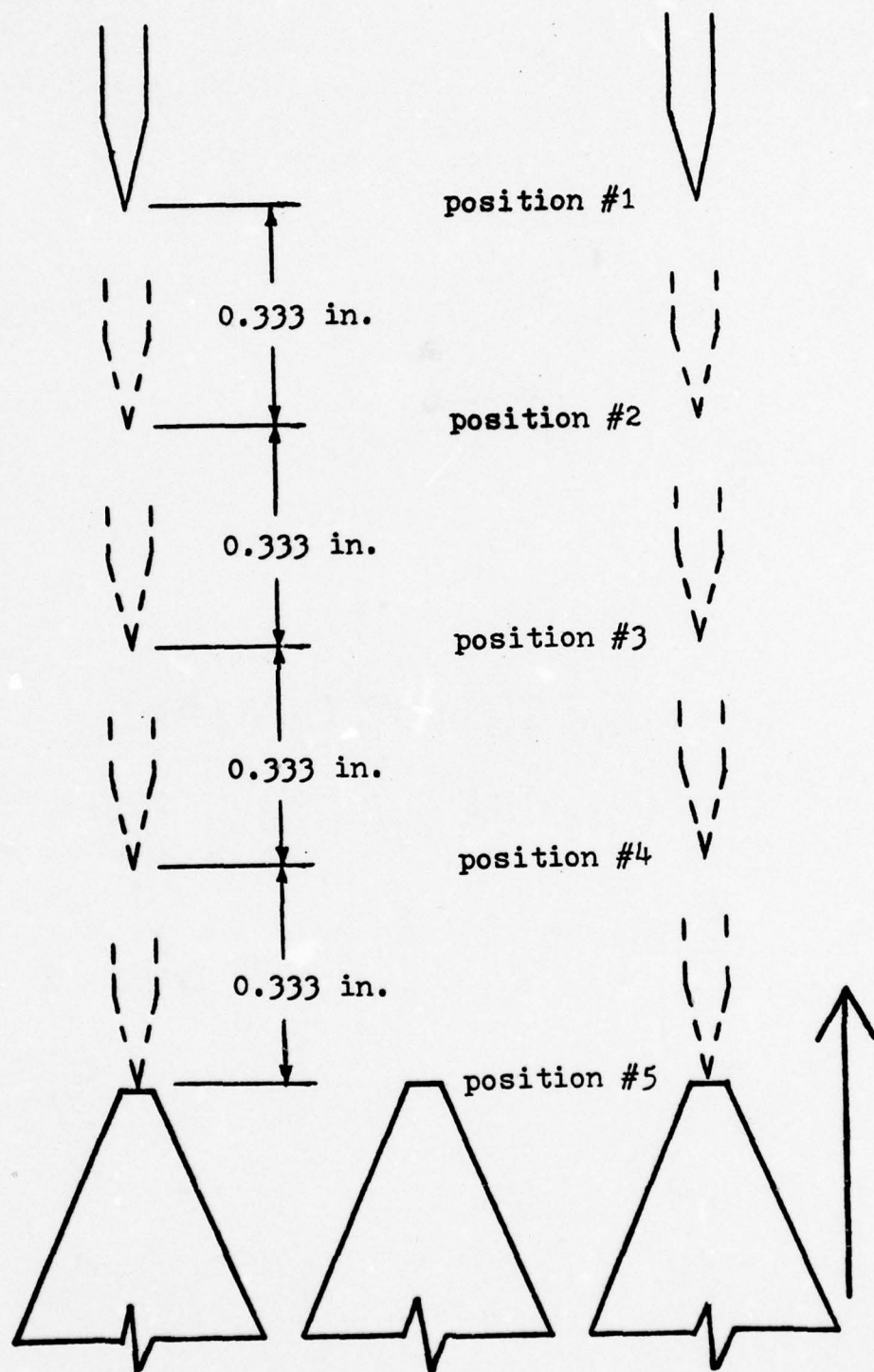
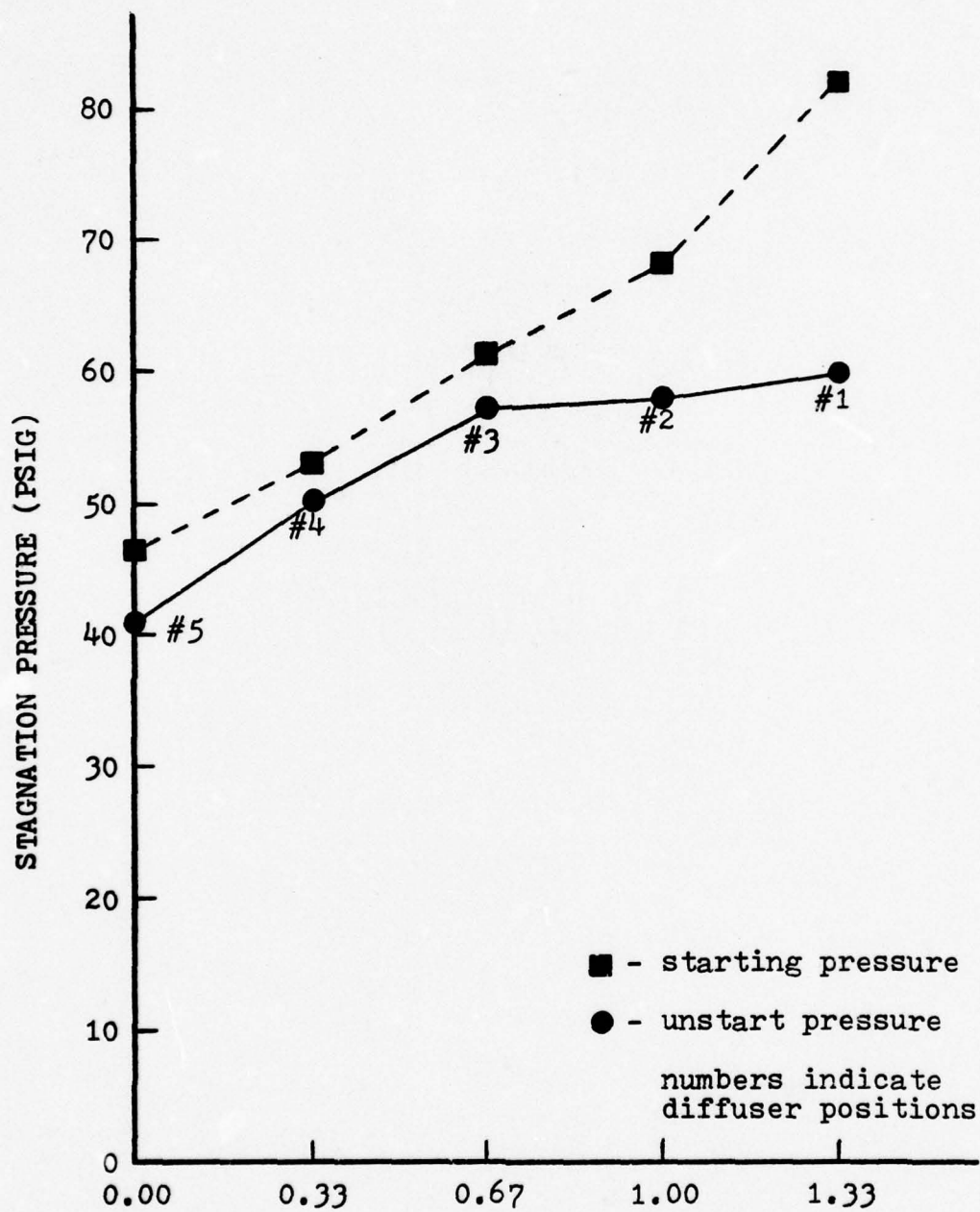


Fig. 11. Diffuser Plane Positions



DISTANCE BETWEEN NOZZLE AND DIFFUSER PLANES, L (INCHES)

Fig. 12. Variation of Start/Unstart Pressures with L

starting pressure was observed between positions one and two. The reduction in unstart pressure was 18 psig between positions one and five. The greatest pressure reduction occurred between positions four and five. Once started, system operation was stable at pressures between the start and unstart pressures. A stable operating range of 22 psig was observed at position one between the start and minimum operating pressures. This operating range was reduced to 2 psig at position four. The system maintained stable operation at all available pressures greater than the minimum starting pressure.

At position two, the diffuser leading edges were in the immediate vicinity of the intersection of alternate nozzle trailing edge shocks. The region is circled in Fig 13 . At this position, the entire wake flow of nozzle vane number 20 remained subsonic after the assembly was started for 50 per cent of the test runs. Figure 14 depicts this subsonic wake. At the same time, the remainder of the system consistently started. Operation of the system was stable and remained stable as line pressure was decreased to system unstart. System start and unstart pressures were the same for all test runs at this position. This phenomenon appeared to be a function of the geometric position of the diffuser leading edge relative to the shock intersection. Comparison of schlieren photographs

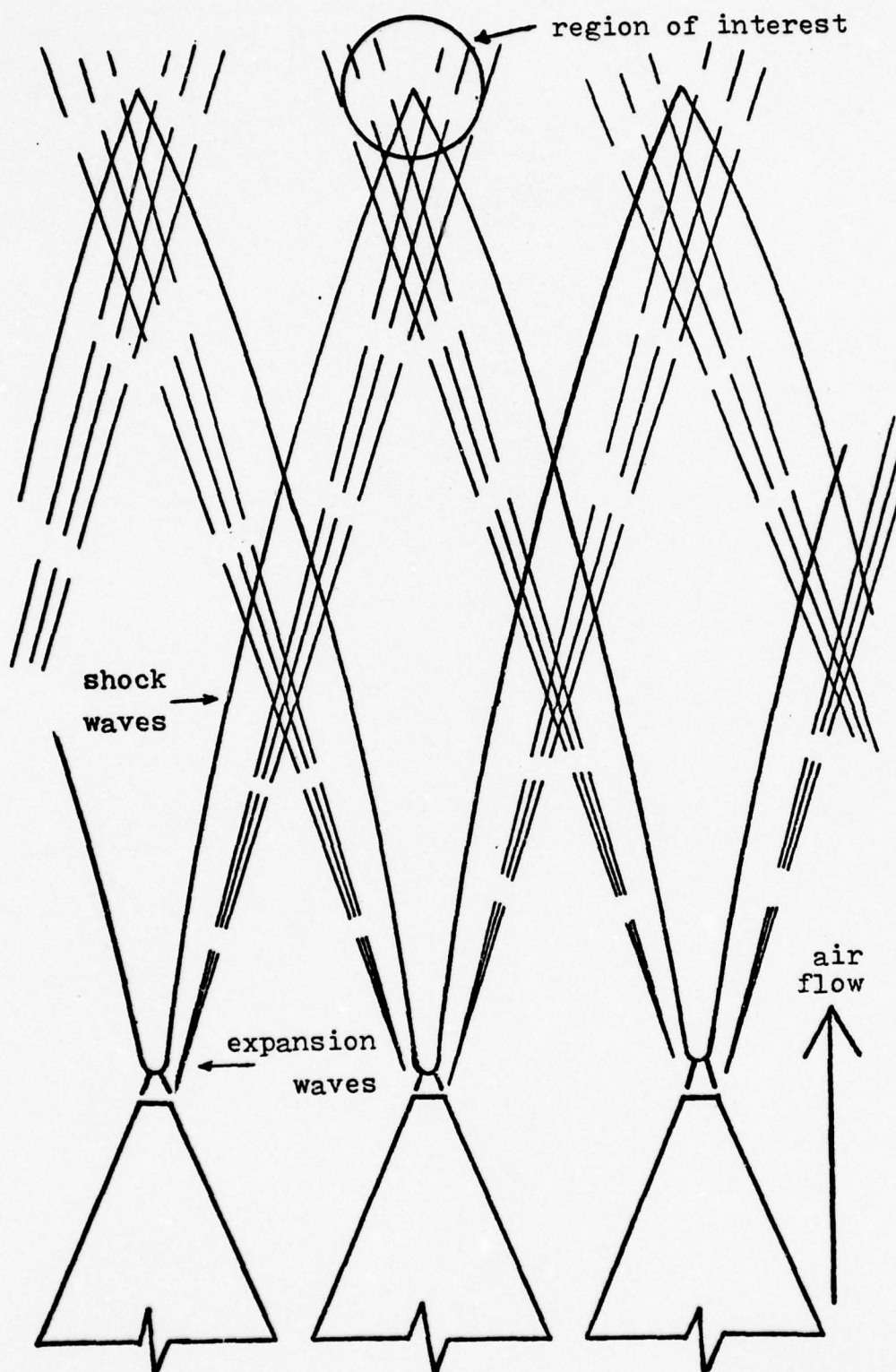


Fig. 13. Shock Expansion Pattern at Nozzle Trailing Edge

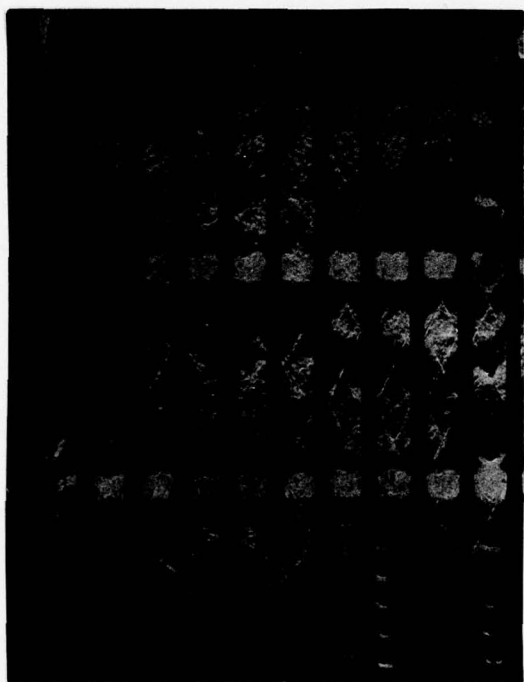


Fig. 14. Schlieren Photograph of Subsonic Wake from
Nozzle Vane Number 20 , $L = 1.000$ inches, $P_o = 68$ psig

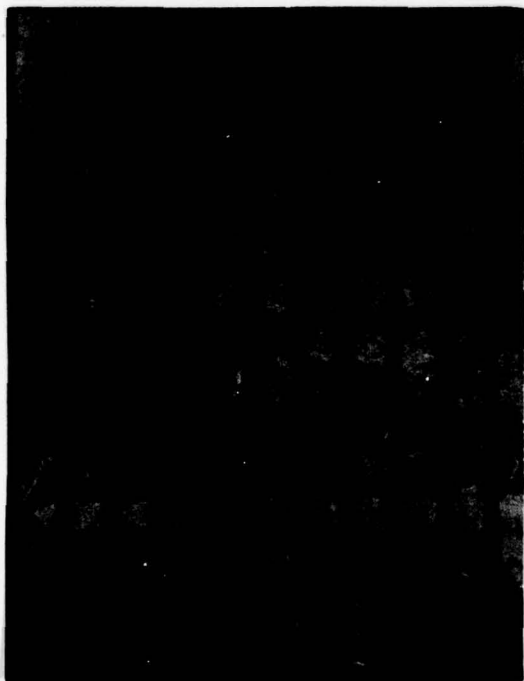


Fig. 15. Schlieren Photograph of Full Cavity Start,
 $L = 1.000$ inches, $P_o = 68$ psig

taken when this phenomenon did and did not occur (Fig 14 and Fig 15), show that all of the diffuser vanes except number 10 were slightly offset to one side of the shock intersection. At diffuser vane number 10 , they intersect precisely at the leading edge. During cavity start, the ability of this intersection to initially stabilize was the determining factor in whether this wake remained supersonic or subsonic. Hence, to assure a stable cavity start, the diffuser leading edges should not be in the immediate vicinity of major shock intersections.

All nozzle inlets were exposed to the same uniform stilling chamber flow conditions. Flow perturbations were not introduced to the stilling chamber to study their effect upon the starting performance.

Static Pressure Variation in the Diffuser

The type diffuser used for this study is classically referred to as a normal shock diffuser (ref 5:130, 11:144). However, schlieren photographs reveal only oblique shocks and a region of transition. This region of transition is a wide region of varying density gradient and is clearly visible in Fig 10, 14, and 15 . Flow entering the region was supersonic, and flow exiting the region was subsonic. Pressure data, as shown in Fig 16, 17, 18, 19, and 20 , shows a region of decreased pressure, or at least a pressure plateau at

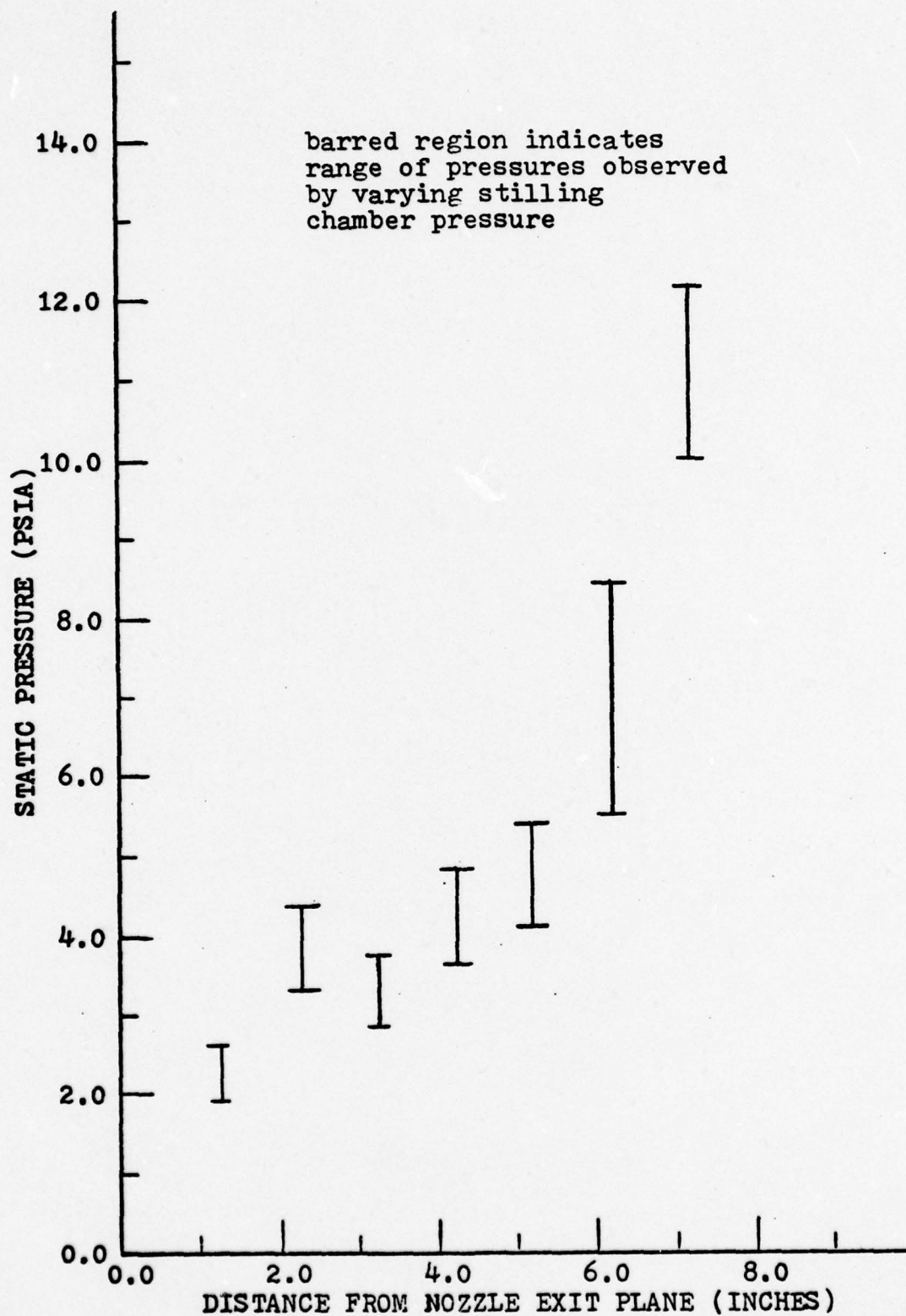


Fig. 16. Diffuser Static Pressure Variation, $L = 1.333$ in.

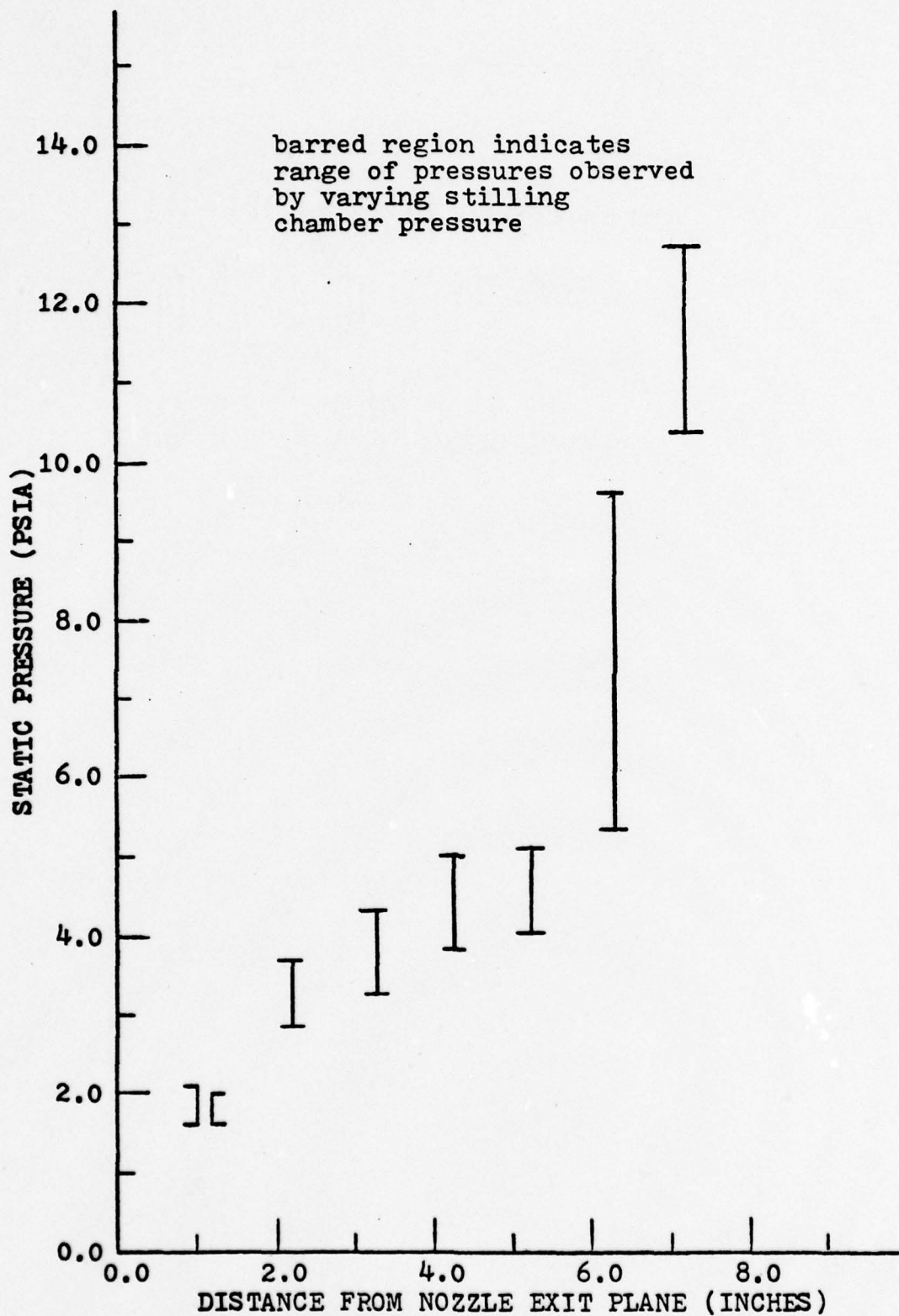


Fig. 17. Diffuser Static Pressure Variations, $L = 1.000$ in.

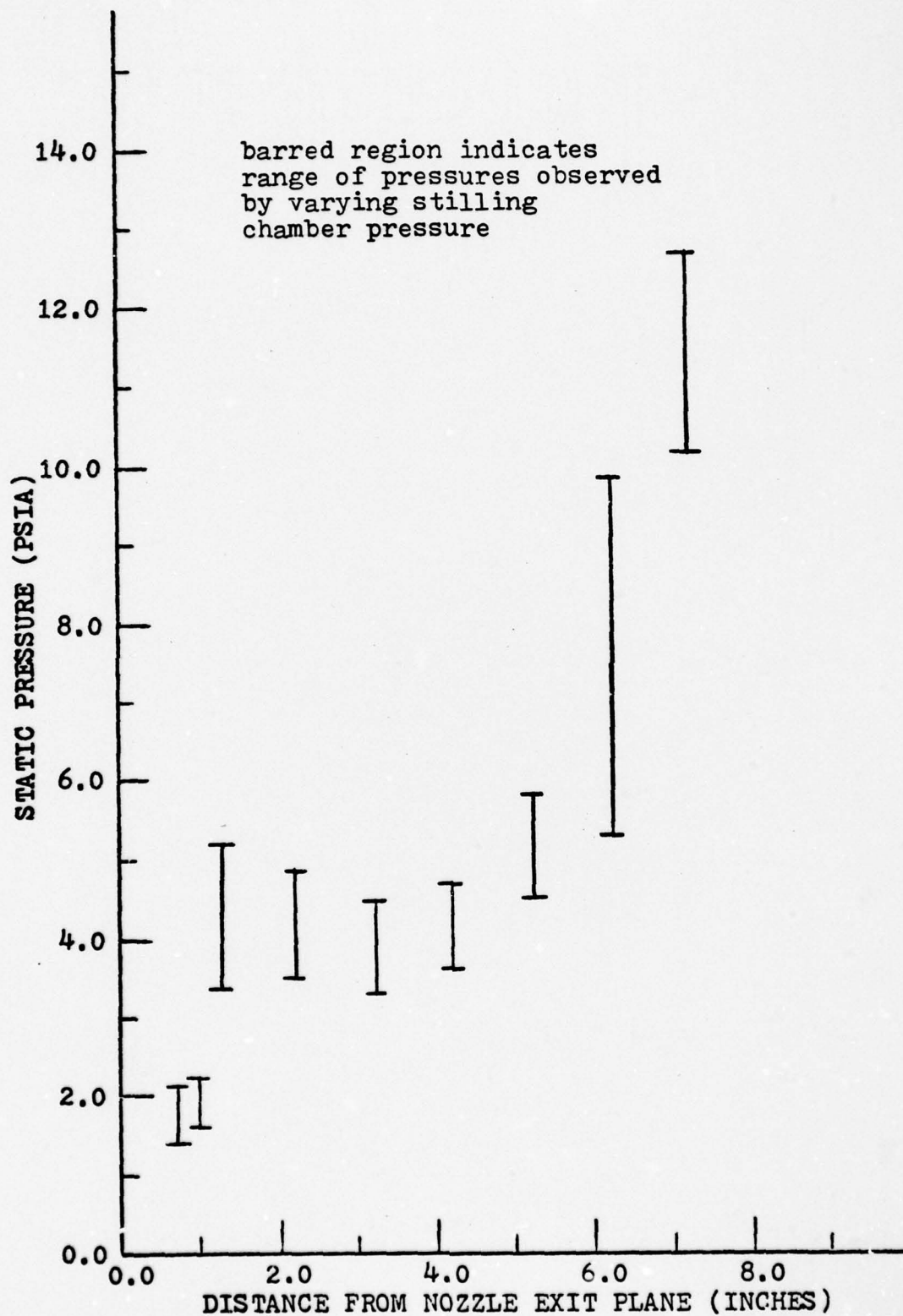


Fig. 18. Diffuser Static Pressure Variations, $L = 0.667$ in.

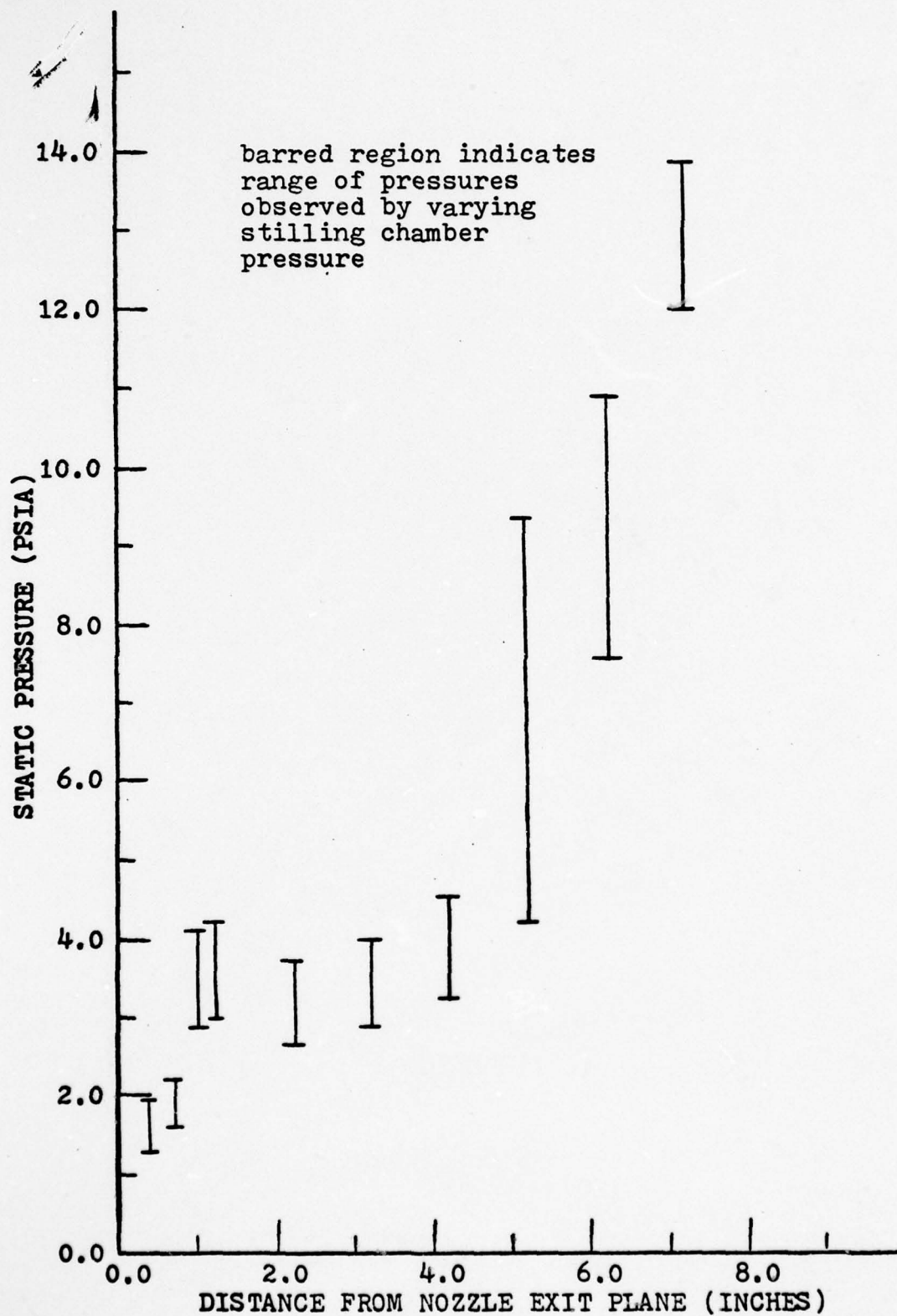


Fig. 19. Diffuser Static Pressure Variations, $L = 0.333$ in.

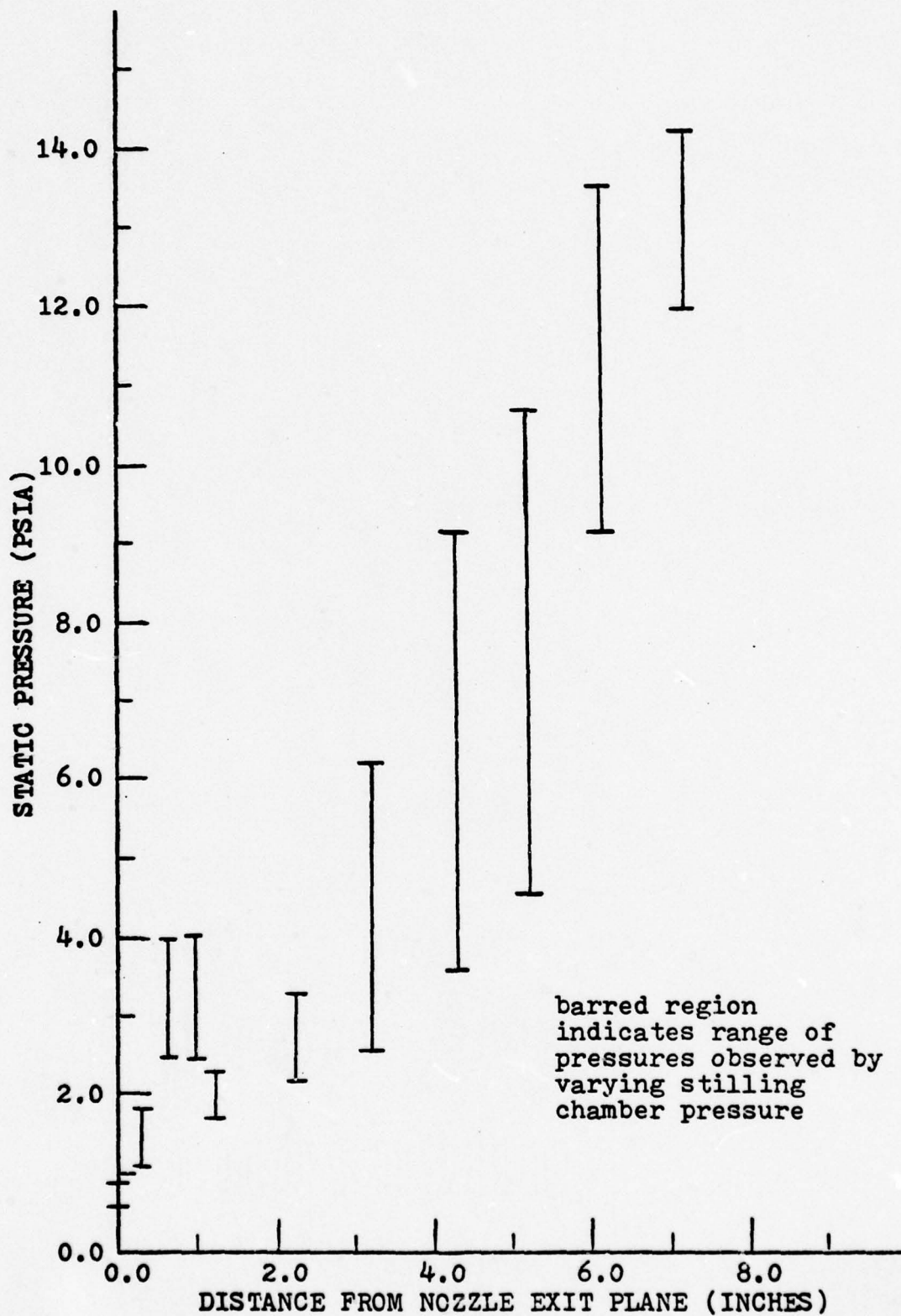


Fig. 20. Diffuser Static Pressure Variations, $L = 0.000$ in.

L = 1.000 inch, in the diffuser passage. (Additional pressure data is shown in appendix A.) The reason for this was that the flow passed through a Prandtl-Meyer expansion emanating from the inlet corner of the diffuser vanes. If this phenomenon could be eliminated or its effects reduced, the starting pressure probably could be lowered, and the diffuser length could be shortened.

V. Conclusions and Recommendations

As a result of this study, the following conclusions and recommendations have been made.

Conclusions

1. A test cavity with a variable position diffuser started and maintained stable operation at significantly lower pressures than did the same assembly using a fixed diffuser.
2. The stagnation pressure required to start the test cavity was reduced as the diffuser entrance plane approached the nozzle exit plane.
3. The minimum operating pressure of the test cavity was also reduced as the diffuser entrance plane approached the nozzle exit plane.
4. Once started, operation of the rest cavity was stable at all pressures greater than the minimum operating pressure.

Recommendations

1. A study of boundary layer growth in the diffuser passages would be of interest. It is possible that limited use of boundary layer control in the diffuser could significantly reduce the stagnation pressure required to start the test cavity.
2. Other geometric configurations of the diffuser

should be studied to determine which configuration yields the best pressure recovery in the shortest length. In a study of this nature, the number of nozzles and the distance between the nozzle exit plane and diffuser entrance plane should remain constant.

Bibliography

1. Bevan, Steven B. Flow Characteristics In A Gas Dynamic Laser Type Multiple Nozzle-Diffuser Assembly. Unpublished Thesis. Wright-Patterson Air Force Base, Ohio: Air Force Institute of Technology, 1974.
2. Christiansen, Walter H. Problems Associated With The Improvement of the Gas Dynamic Laser. Grant Number DA-ARO-D-31-124-72-G8, U.S. Army Research Office, Durham: 31 July 1972.
3. Clawson, David G. Investigation of Diffusers for Gas Dynamic Laser Nozzles. Unpublished Thesis. Wright-Patterson Air Force Base, Ohio: Air Force Institute of Technology.
4. Keenan, Joseph H. and Joseph Kaye. Gas Tables. New York: John Wiley and Sons, 1948.
5. Liepmann, H.W. and A. Roshko. Elements of Gasdynamics. New York: John Wiley and Sons, May, 1967.
6. McQuarrie, D.A. Statistical Thermodynamics. New York: Harper and Row, 1973.
7. Mensing, Arthur E., et al. Investigations of the Effect of Combustor Geometry and End Nozzle Flow on the Performance of GDL Type Diffusers. Contract No. F33615-73-C-4077, U.S. Air Force Aerospace Research Laboratories, Wright-Patterson Air Force Base, Ohio: November, 1973.
8. Nuttbrock, Dennis L. Investigation of the Performance of a Variable Area Diffuser for Gas Dynamic Lasers. Unpublished Thesis. Wright-Patterson Air Force Base, Ohio: Air Force Institute of Technology, June, 1974.
9. Patel, C.K.N. "High-Power Carbon Dioxide Lasers" Scientific American, 219: 22-33 (August, 1968).
10. Sarner, Stanley F. Propellant Chemistry. New York: Reinhold Publishing Corporation, 1966.
11. Shapiro, Asher H. The Dynamics and Thermodynamics of Compressible Fluid Flow. New York: The Ronald Press, 1953.
12. Vincenti, W.G. and C.H. Kruger. Introduction to Physical Gas Dynamics. New York: Wiley, 1965.

Appendix A

Axial Variation of Static Pressure in Nozzle Trailing
Edge Wakes, Nozzle Center Streamline, and Diffuser
Center Streamline

Axial Variation of Static Pressure in Nozzle Trailing
Edge Wakes, Nozzle Center Streamline, and Diffuser
Center Streamline

The following tables and figures show static pressure variations, in psia, in the nozzle center streamline, nozzle trailing edge wakes, and diffuser center streamlines. Each table and figure displays data at one value of L only. Data is shown as a variation of stilling chamber pressure (psig) versus streamwise distance, x (inches), at the specified value of L. All data displayed was obtained from a steady state fully started test cavity. All manometer readings were repeatable ± 0.05 inches of mercury. Each bar in Fig 21-26 indicates the range of static pressures obtained at a particular pressure tap by varying the stilling chamber pressure and holding L constant. Figures 16-26 graphically represent data shown in tables I-V.

Table I

Static Pressure Variation in the Test Cavity

L = 1.333 in.

tap #	P _o (psig)					
	60	65	70	75	80	82
1.	1.779	1.779	1.877	2.049	2.417	2.147
2.	1.189	1.263	1.337	1.410	1.533	1.508
3.	1.459	1.558	1.680	1.779	2.000	1.852
4.	1.435	1.582	1.680	1.828	1.926	1.950
5.	1.263	1.386	1.459	1.582	1.705	1.607
6.	0.698	0.796	0.821	0.870	0.944	0.919
7.	1.631	1.779	1.901	2.024	2.171	2.098
8.	1.852	2.000	2.049	2.221	2.343	2.417
9.	1.680	1.779	1.926	2.000	2.196	2.073
10.	1.950	2.073	2.270	2.368	2.564	2.343
11.	3.350	3.620	3.841	4.136	4.381	4.480
12.	2.908	3.105	3.301	3.571	3.768	3.817
13.	3.792	4.038	4.332	4.676	4.922	4.946
14.	4.160	4.455	4.725	5.069	5.413	5.462
15.	8.531	7.942	6.616	5.585	5.683	5.658
16.	12.116	11.994	11.552	11.674	11.134	11.085

pressures shown in psia

barometer = 29.336 in. Hg

Table II
Static Pressures in the Test Cavity
L = 1.000 in.

tap #	60	65	68	P _o (psig) 70	75	80
1.	1.715	1.739	1.837	1.862	2.009	2.107
2.	1.223	1.297	1.322	1.420	1.469	1.616
3.	1.371	1.469	1.567	1.567	1.665	1.960
4.	1.469	1.543	1.567	1.665	1.764	1.960
5.	1.862	1.911	2.009	2.107	2.255	2.353
6.	0.683	0.757	0.781	0.831	0.880	0.880
7.	1.469	1.592	1.665	1.665	1.813	1.911
8.	1.665	1.739	1.813	1.862	2.009	2.058
9.	1.616	1.715	1.764	1.813	1.960	2.058
10.	1.616	1.715	1.715	1.715	1.911	2.009
11.	2.893	3.041	3.188	3.237	3.483	3.679
12.	3.384	3.581	3.728	3.777	4.023	4.317
13.	3.875	4.121	4.268	4.416	4.612	4.907
14.	4.023	4.170	4.317	4.416	4.710	5.005
15.	9.621	9.179	7.517	6.626	5.152	5.496
16.	12.617	12.666	12.323	11.979	12.077	11.046

pressures shown in psia

barometer = 29.204 in. Hg

Table III

Static Pressures in the Test Cavity

L = 0.667 in.

tap #	P _o (psig)					
	60	62	65	70	75	80
1.	1.776	1.776	1.874	1.972	2.071	2.267
2.	1.187	1.187	1.481	1.383	1.432	1.530
3.	1.383	1.432	1.481	1.678	1.678	1.874
4.	2.021	2.120	2.169	2.365	2.463	2.660
5.	2.414	2.463	2.562	2.807	2.758	3.102
6.	0.745	0.745	0.745	0.843	0.941	1.039
7.	1.530	1.579	1.579	1.825	1.874	2.120
8.	1.678	1.776	1.776	1.923	2.021	2.169
9.	1.629	1.727	1.727	1.972	1.972	2.218
10.	3.593	3.691	3.888	4.526	4.084	5.263
11.	3.740	3.789	3.937	4.281	4.379	4.821
12.	3.347	3.446	3.593	4.084	3.937	4.575
13.	3.642	3.740	3.839	4.231	4.231	4.772
14.	4.526	4.525	4.821	5.165	5.066	5.803
15.	9.976	9.339	8.750	6.982	5.312	5.901
16.	12.629	12.482	12.138	12.089	11.451	11.107

pressures shown in psia

barometer = 29.028 in. Hg

Table IV

Static Pressure Variation in the Test Cavity

L = 0.333 in.

tap #	53	55	60	P _o (psig) 65	70	75	80
1.	1.573	1.622	1.819	1.868	2.015	2.163	2.261
2.	1.082	1.131	1.180	1.279	1.377	1.426	1.573
3.	1.917	2.015	2.163	2.310	2.457	2.654	2.801
4.	2.359	2.408	2.506	2.703	2.899	3.047	3.243
5.	2.654	2.752	2.948	3.096	3.341	3.587	3.783
6.	0.689	0.738	0.738	0.837	0.886	0.886	0.935
7.	1.328	1.426	1.475	1.573	1.721	1.819	1.966
8.	1.622	1.573	1.721	1.819	1.966	2.064	2.212
9.	2.899	2.948	3.145	3.390	3.636	3.832	4.127
10.	2.997	3.047	3.390	3.489	3.832	4.029	4.225
11.	2.654	2.703	2.948	3.145	3.341	3.538	3.734
12.	2.899	2.997	3.145	3.390	3.587	3.783	4.029
13.	3.292	3.292	3.489	3.783	3.980	4.274	4.569
14.	9.382	8.645	6.042	4.274	4.569	4.815	5.060
15.	11.887	11.739	10.806	10.020	9.529	9.235	7.417
16.	13.704	13.556	13.114	12.869	12.672	12.379	12.034

pressures shown in psia

barometer = 29.216 in. Hg

Table V

Static Pressure Variation in the Test Cavity

L = 0.000 in.

tap #	45	50	55	60	65	70	75	80
1.	1.434	1.483	1.581	1.729	1.827	1.974	2.072	2.220
2.	1.336	1.434	1.581	1.729	1.876	1.974	2.122	2.269
3.	2.023	2.220	2.367	2.564	2.711	2.907	3.104	3.300
4.	2.023	2.171	2.367	2.514	2.613	2.809	3.006	3.104
5.	2.760	3.055	3.251	3.497	3.742	4.028	4.282	4.528
6.	0.599	0.599	0.697	0.746	0.746	0.845	0.894	0.943
7.	1.188	1.238	1.336	1.483	1.483	1.680	1.778	1.876
8.	2.564	2.760	2.907	3.202	3.349	3.595	3.791	3.988
9.	2.514	2.711	2.907	3.104	3.300	3.595	3.791	4.037
10.	1.680	1.729	1.876	2.023	2.072	2.220	2.318	2.367
11.	2.220	2.318	2.514	2.711	2.907	3.006	3.202	3.398
12.	6.149	2.662	2.858	3.055	3.202	3.398	3.595	3.840
13.	9.046	7.524	4.037	3.644	3.840	4.135	4.332	4.626
14.	11.600	10.421	9.095	8.457	7.180	4.970	4.528	4.724
15.	13.466	12.680	12.140	11.796	11.109	10.421	10.028	9.194
16.	14.203	13.957	13.663	13.368	12.975	12.828	12.582	11.993

pressures shown in psia

barometer = 29.134 in. Hg

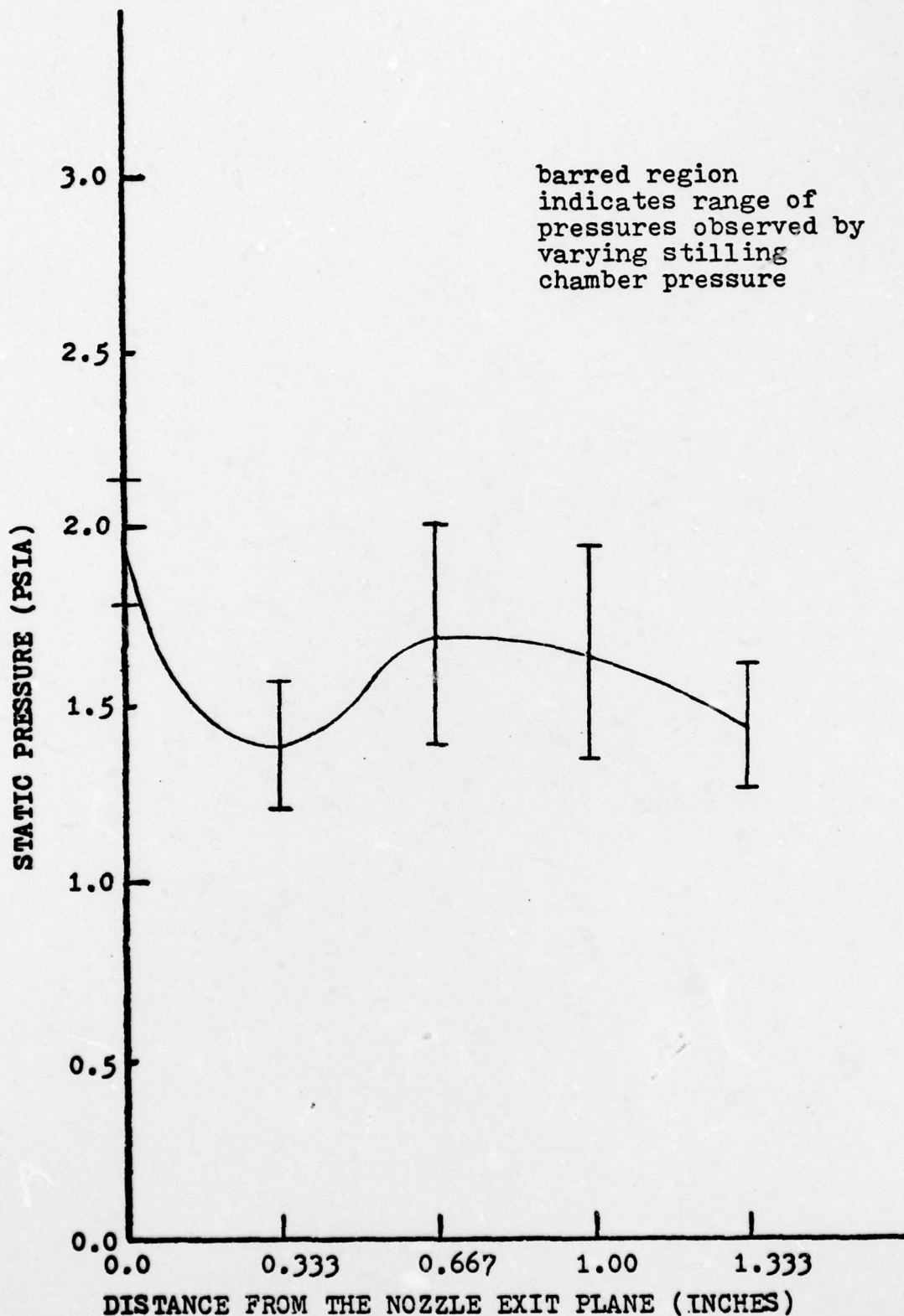


Fig. 21. Nozzle Flow Static Pressure Variation, $L = 1.333$ in.

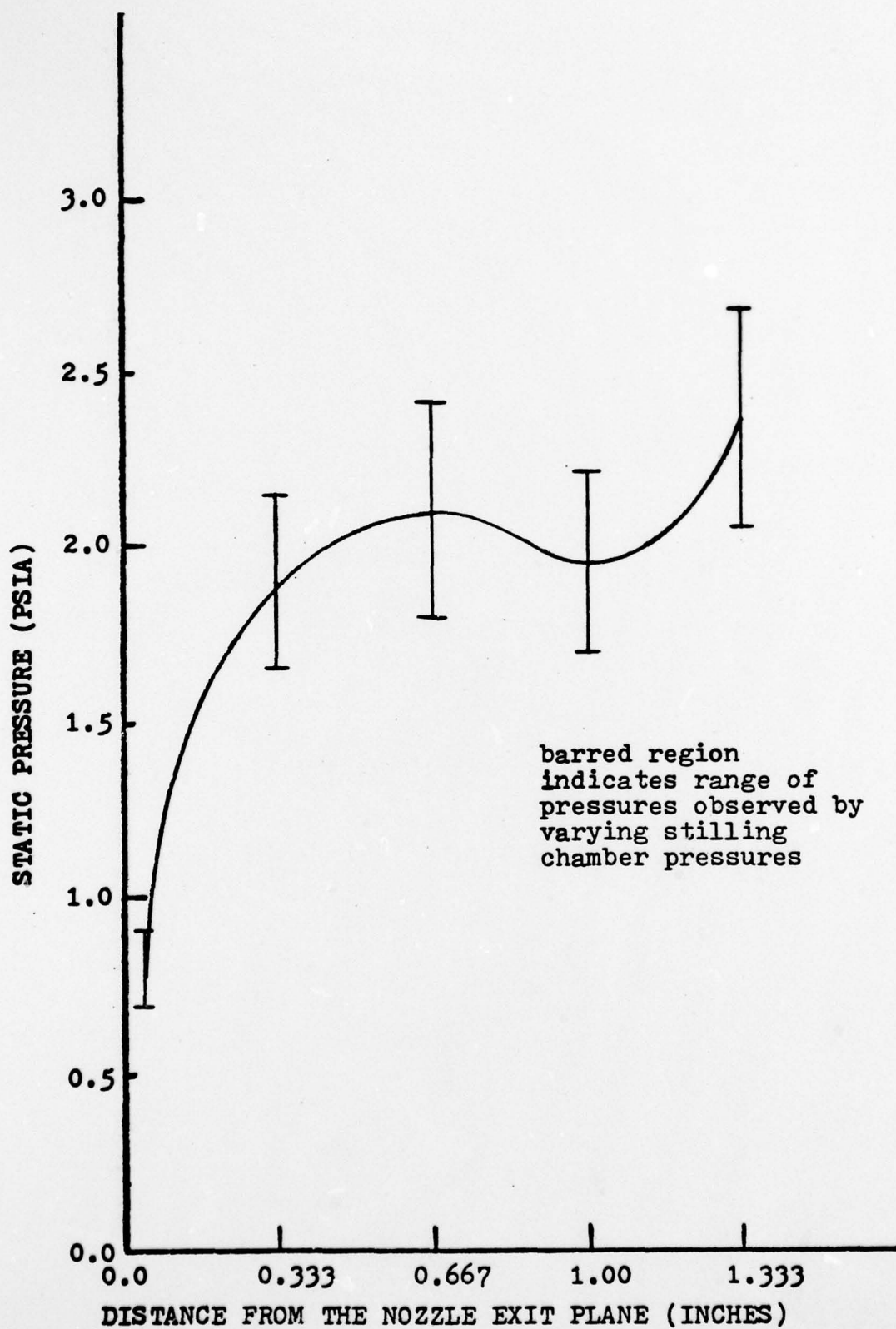


Fig. 22 . Wake Flow Static Pressure Variation, $L = 1.333$ in.

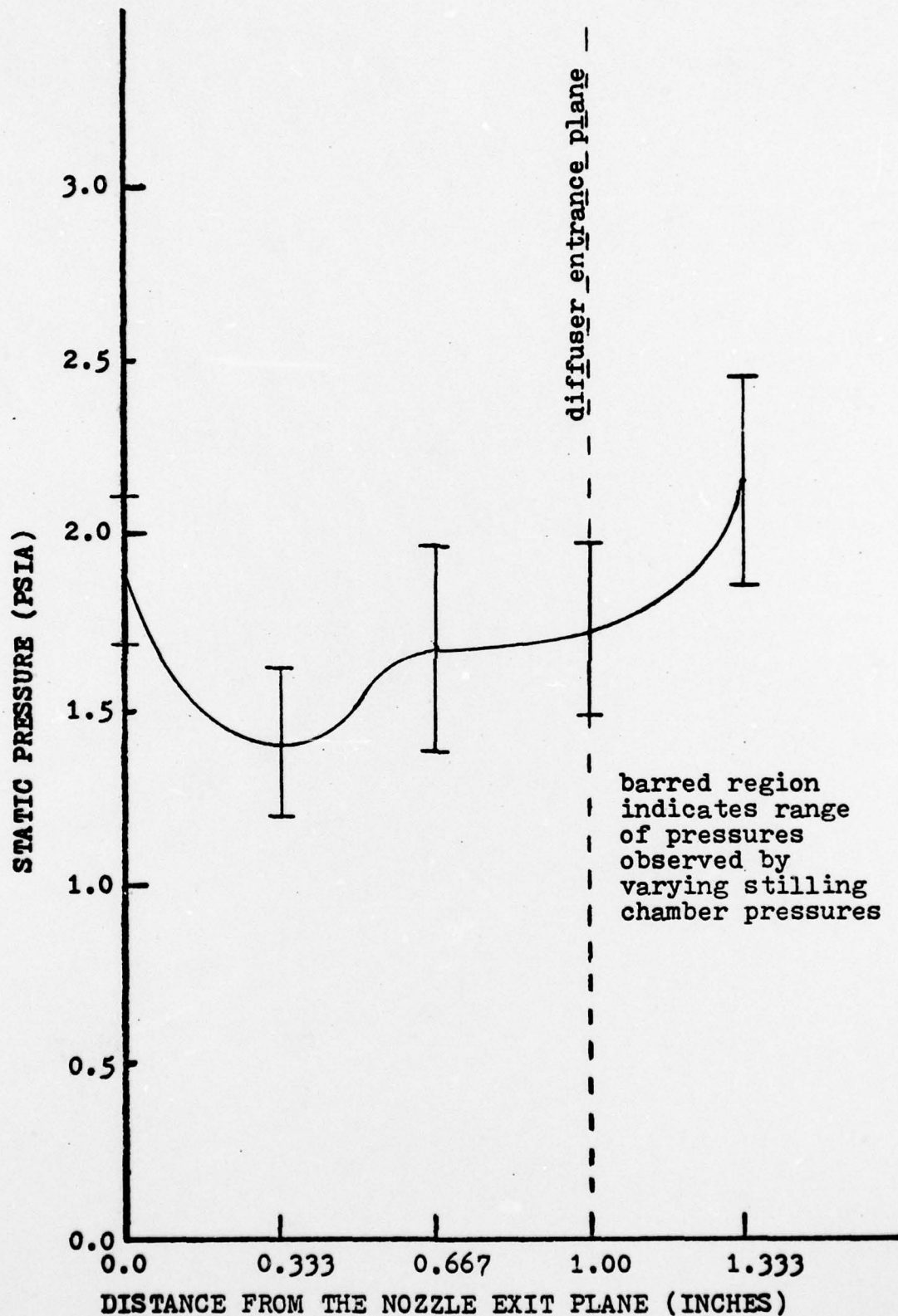


Fig. 23. Nozzle Flow Static Pressure Variation, $L = 1.000$ in.

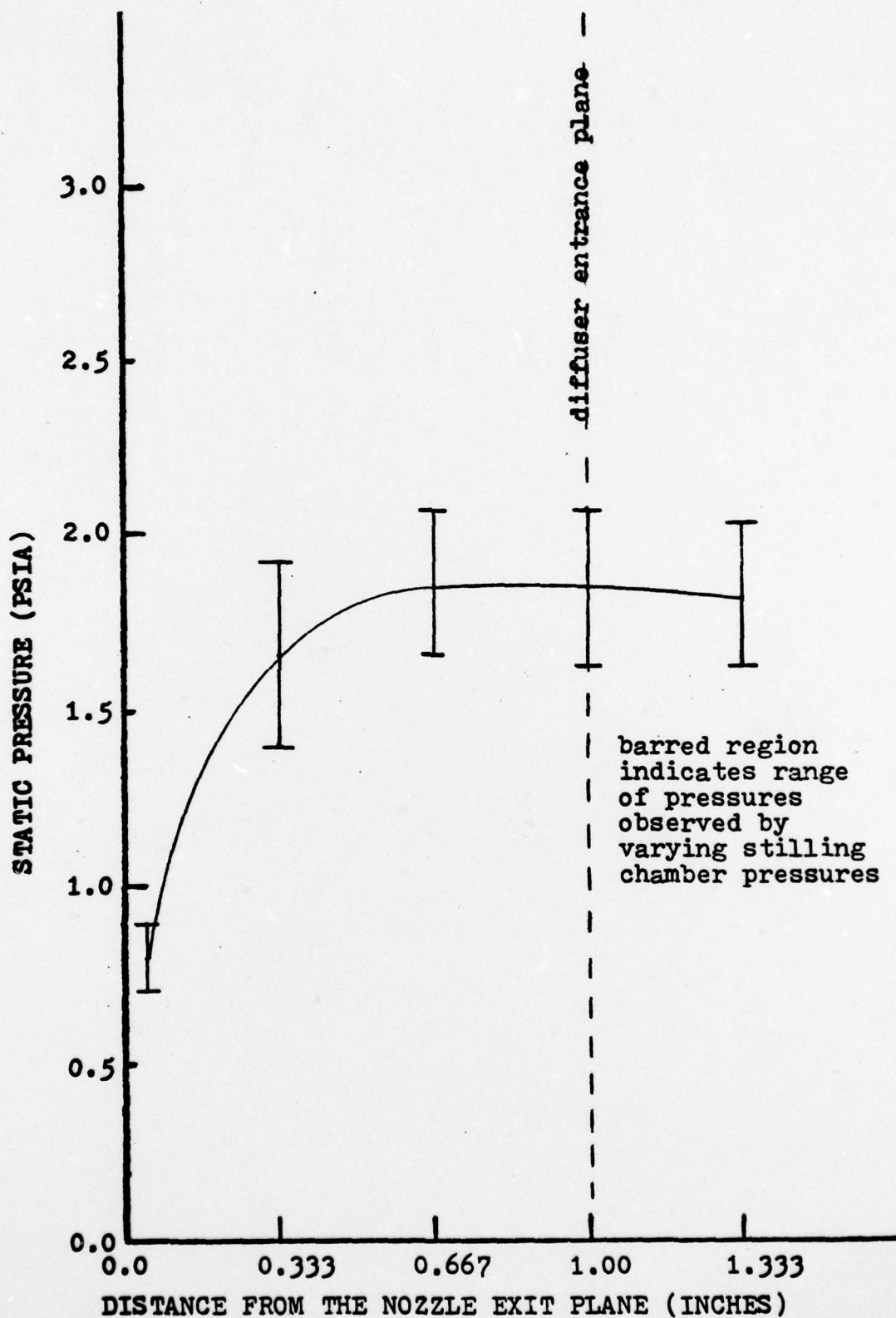


Fig. 24. Wake Flow Static Pressure Variation, $L = 1.000$ in.

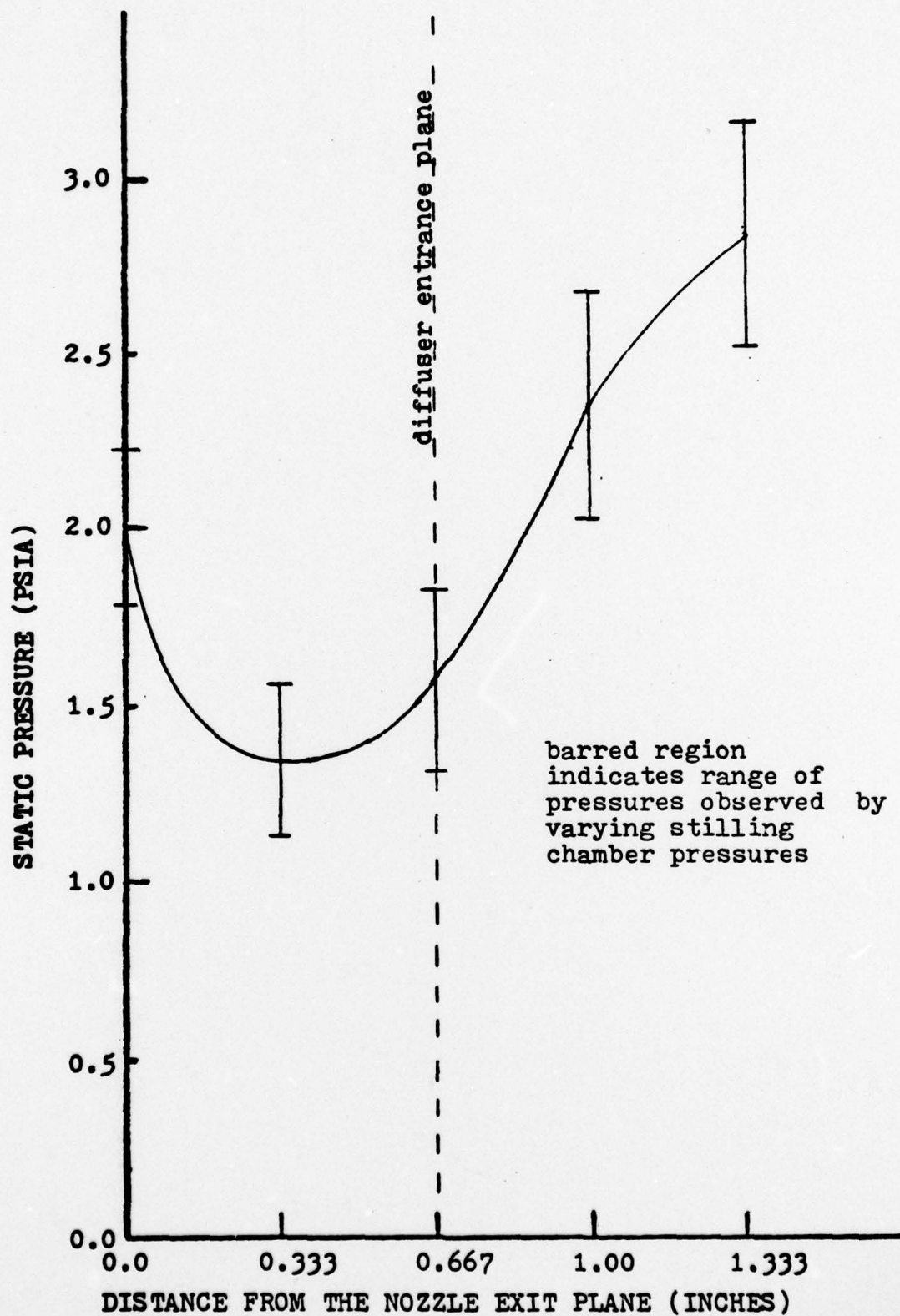


Fig. 25. Nozzle Flow Static Pressure Variation, $L = 0.667$ in.

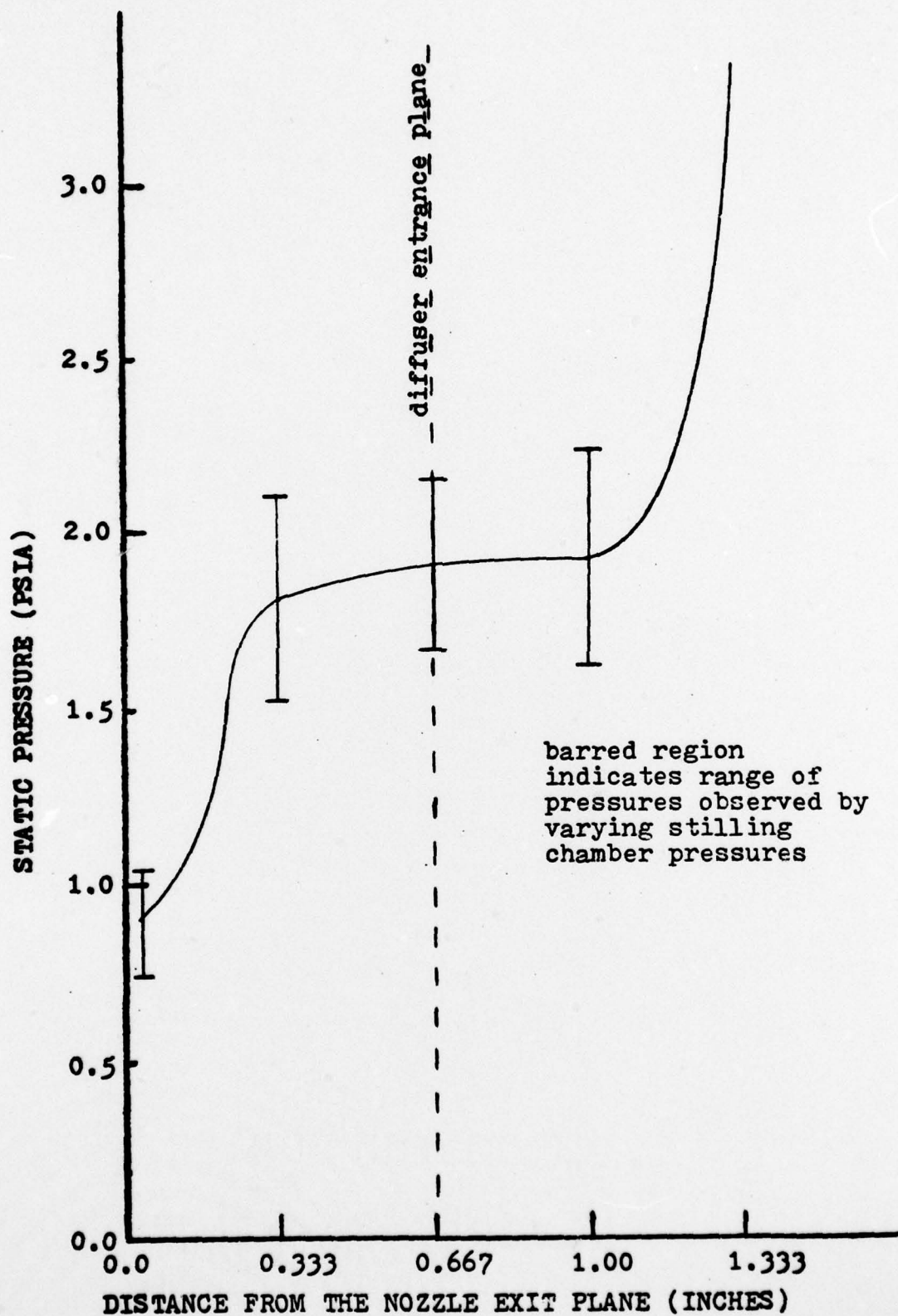


Fig. 26 . Wake Flow Static Pressure Variations, $L = 0.667$ in.

Vita

Jeffrey L. Kiner was born 6 August 1947 in Prophetstown, Illinois, the son of Roland D. and Lois M. Kiner. He graduated from Prophetstown High School in 1965. He graduated from the University of Illinois in 1970 with a Bachelor of Science degree in Aeronautical and Astronautical Engineering. He completed navigator and electronic warfare training at Mather AFB, California, and was assigned to flying in EB-66 aircraft at Korat Royal Thai Air Force Base, Thailand. He entered the Air Force Institute of Technology from an assignment as Remote Control Officer in DC-130 aircraft at Davis-Monthan AFB, Arizona. His assignment upon completion of the AFIT program is at Kirtland AFB, New Mexico, in the Air Force Weapons Laboratory (AFSC).

Permanent address: P.O.Box 44

Prophetstown, Illinois

This thesis was typed by the author.

unclassified

SECURITY CLASSIFICATION OF THIS PAGE (When Data Entered)

14 REPORT DOCUMENTATION PAGE		READ INSTRUCTIONS BEFORE COMPLETING FORM
1. REPORT NUMBER AFIT/GAE/AA/77D-5	2. GOVT ACCESSION NO.	3. REPORT, CONTRACT, OR GRANT NUMBER <i>Master's Thesis</i>
4. TITLE (and Subtitle) FLOW CHARACTERISTICS IN A TWO-DIMENSIONAL MULTIPLE-NOZZLE MULTIPLE-DIFFUSER ASSEMBLY		5. TYPE OF REPORT & PERIOD COVERED MS Thesis
6. PERFORMING ORG. REPORT NUMBER		7. CONTRACT OR GRANT NUMBER(s)
8. AUTHOR(s) Jeffrey L. Kiner Captain USAF		9. PROGRAM ELEMENT, PROJECT, TASK AREA & WORK UNIT NUMBERS
10. PERFORMING ORGANIZATION NAME AND ADDRESS Air Force Institute of Technology (AFIT-EN) Wright-Patterson AFB, Ohio 45433		11. REPORT DATE Dec 1977
12. CONTROLLING OFFICE NAME AND ADDRESS Air Force Weapons Laboratory (AFSC) Kirtland AFB, New Mexico 87115		13. NUMBER OF PAGES 7262p.
14. MONITORING AGENCY NAME & ADDRESS (if different from Controlling Office)		15. SECURITY CLASS. (if different from Unclassified)
16. DISTRIBUTION STATEMENT (of this Report) Approved for public release; distribution unlimited		
17. DISTRIBUTION STATEMENT (of the abstract entered in Block 20, if different from Report)		
18. SUPPLEMENTARY NOTES Approved for public release; IAW AFR 190-17 JERRAL F. GUESS, Captain, USAF Director of Information		
19. KEY WORDS (Continue on reverse side if necessary and identify by block number) Laser, Multiple-Diffuser flow, Starting, Variable Geometry, Multiple-Nozzle flow, Nozzle wakes		
20. ABSTRACT (Continue on reverse side if necessary and identify by block number) Pressure measurements and schlieren photographs were used to study the flow characteristics in a two-dimensional multiple-nozzle multiple-diffuser assembly. The assembly consisted of 29 full nozzles with a half nozzle at each end of the array. The contoured nozzles were designed for an ideal Mach number of 3.23. Fourteen axial diffuser vanes provided 15 diffuser passages. Flow characteristics were studied at five positions of the diffuser entrance plane with respect to the nozzle exit		

DD FORM 1 JAN 73 1473

EDITION OF 1 NOV 65 IS OBSOLETE

unclassified

SECURITY CLASSIFICATION OF THIS PAGE (When Data Entered)

012225

next
Page

unclassified

SECURITY CLASSIFICATION OF THIS PAGE(When Data Entered)

plane. Air at 80F and a maximum of 118 psig was passed through the nozzles into a constant area region then through the diffusers to ambient conditions. The test cavity start and unstart pressures decreased as the diffuser entrance plane approached the nozzle exit plane. A diffuser leading edge in the immediate vicinity of a major alternate nozzle trailing edge shock intersection resulted in a flow instability during cavity start. This instability resulted in a subsonic wake in the test cavity after cavity start.

unclassified

SECURITY CLASSIFICATION OF THIS PAGE(When Data Entered)